



Kampweg 5
P.O. Box 23
3769 ZG Soesterberg
The Netherlands

www.tno.nl

T +31 346 35 62 11
F +31 346 35 39 77
Info-DenV@tno.nl

TNO report

TNO-DV 2008 A126

Models & Methods in SCOPE

A status report

Date	April 2008
Author(s)	E.M. Ubink, MSc Dr W.A. Lotens R.F. Aldershoff, MSc
Classification report	Ongerubriceerd
Classified by	Ikol J. Kerkhof
Classification date	15 February 2008
Title	Ongerubriceerd
Managementuitreksel	Ongerubriceerd
Abstract	Ongerubriceerd
Report text	Ongerubriceerd
Copy no	7
No. of copies	20
Number of pages	59 (excl. RDP & distributionlist)

The classification designation Ongerubriceerd is equivalent to Unclassified, Stg. Confidentieel is equivalent to Confidential and Stg. Geheim is equivalent to Secret.

All rights reserved. No part of this report may be reproduced in any form by print, photoprint, microfilm or any other means without the previous written permission from TNO.

All information which is classified according to Dutch regulations shall be treated by the recipient in the same way as classified information of corresponding value in his own country. No part of this information will be disclosed to any third party.

In case this report was drafted on instructions from the Ministry of Defence the rights and obligations of the principal and TNO are subject to the standard conditions for research and development instructions, established by the Ministry of Defence and TNO, if these conditions are declared applicable, or the relevant agreement concluded between the contracting parties.

© 2008 TNO

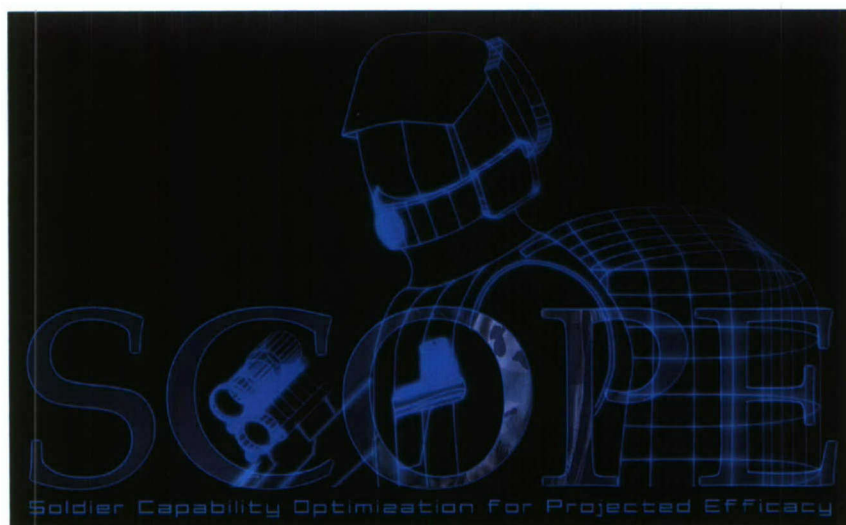
AQ F08-08-05907

20080507050

Modellen & Methoden in SCOPE

Stand van zaken

SCOPE is een simulatie van uitgestegen eenheden ontwikkeld door TNO. In dit rapport wordt een overzicht gegeven van de in SCOPE geïmplementeerde modellen en methoden.



Inleiding

SCOPE is een simulatie van uitgestegen eenheden gericht op het uitvoeren van onderzoek naar operationele effectiviteit. SCOPE bevat een grote verscheidenheid aan modellen, variërend van wapeneffectmodellen tot modellen op het gebied van de fysiologie. In dit rapport wordt een overzicht van al deze modellen gegeven.

Doelstelling

Het doel van dit rapport is tweeledig. Enerzijds biedt het rapport inzicht in de mogelijkheden van SCOPE om operationele vragen mee te beantwoorden. Kortom: de opsomming van modellen biedt impliciet

een indicatie van de inzet-mogelijkheden van SCOPE.

Anderzijds vormt dit rapport, samen met de feitelijke code en andere documentatie, een borging van de kennis die binnen SCOPE ontwikkeld is. Dit rapport kan als zodanig ook gebruikt worden om inzicht te krijgen in de kennis die binnen SCOPE is ontwikkeld, en eventuele mogelijkheden om deze kennis op andere terreinen in te zetten.

Gedrag

Veel van de factoren die van invloed zijn op menselijke prestatie hebben slechts een indirecte invloed via het gedrag. Daarom is binnen SCOPE veel aandacht uitgegaan naar het ontwikkelen van een gedragsmodel

dat geschikt is voor het modelleren van menselijke prestatie.

Situation Awareness

Situation Awareness (SA) is een andere belangrijke factor in menselijk presteren. SCOPE bevat diverse modellen op het vlak van SA, variërend van een model van (subjectieve) dreigingsperceptie, tot een meer technisch radio-propagatie model.

Fysiologie

Vermoeidheid en uitputting kunnen aanzienlijke operationele consequenties hebben. Daarom speelt binnen SCOPE fysiologie een grote rol en is zowel het menselijk thermische systeem als het metabolisme gemodelleerd.

Wapeneffecten

Het SCOPE wapeneffectmodel is geschikt voor zowel direct als indirect vuur en bevat diverse ballistische beschermingstypen. Doordat wapens gedefinieerd worden aan de hand van eigenschappen kunnen eenvoudig nieuwe wapenconcepten gemodelleerd worden.

Contact en rapportinformatie

Kampweg 5
Postbus 23
3769 ZG Soesterberg

T +31 346 35 62 11
F +31 346 35 39 77

Info-DenV@tno.nl

TNO-rapportnummer
TNO-DV 2008 A126

Opdrachtnummer
-

Datum
april 2008

Auteur(s)
drs. E.M. Ubink
dr. W.A. Lotens
drs. R.F. Aldershoff

Rubricering rapport
Ongerubriceerd

PROGRAMMA	PROJECT
Programmabegeleider Ikol J. Kerkhof, Bureau SMP	Projectbegeleider maj H.J. van den Brink, Mindef/DS/CLAS/OTCO/OTCMan
Programmaleider dr. ir. A.A. Woering, TNO Defensie & Veiligheid	Projectleider drs. R.F. Aldershoff, TNO Defensie & Veiligheid
Programmatitel Soldaat Optreden	Projecttitel Scope Consolidatie
Programmanummer V707	Projectnummer 032.13114
Programmaplanning Start 1 januari 2007 Gereed 31 december 2010	Projectplanning Start 1 januari 2007 Gereed 31 december 2008
Frequentie van overleg Niet van toepassing	Projectteam dr. ir. A.A. Woering drs. R.F. Aldershoff dr. W.A. Lotens drs. E.M. Ubink

Summary

TNO has developed SCOPE, a simulation of dismounted soldier operations. SCOPE is used for research in the field of operational performance. Operational performance depends on many factors, varying from climate and terrain characteristics to group dynamics and equipment. SCOPE contains models representing many of these factors. This report gives an overview of the current status of these models. The models and variables in SCOPE can be grouped into four main categories: models related to behaviour, models related to situational awareness (SA), models related to physiology and models related to weapons effects.

The behaviour model in SCOPE is based on the pandemonium model, with several behaviour components competing over a limited set of resources, to control behaviour. The behaviour model incorporates multi-tasking and stress and strain effects. The SA related models and variables in SCOPE are concerned with visual perception, identification, (subjective) threat perception and (radio) communication. This includes various models of hardware such as vision devices and radios. SCOPE contains several physiological models. There is a model of the human thermal system that incorporates the thermal effects of clothing, climate and physical activity and is capable of predicting thermal stress. A model of the metabolic system is used to predict water and food consumption and fatigue and exhaustion effects. The latter is also predicted with the simple model of sleep deprivation that is incorporated into SCOPE. Finally, the weapon effects model is used for ballistic engagements and can handle a wide variety of both weapons and ballistic protections.

Contents

	Managementuitbreksel.....	2
	Summary	4
1	Introduction	6
1.1	Overview	6
2	Behaviour	7
2.1	Human Behaviour Modelling.....	7
2.2	Pandemonium model of letter recognition.....	8
2.3	The CHAOS behaviour framework.....	8
2.4	Group dynamics and readiness.....	14
2.5	Future Work.....	16
3	Situation Awareness.....	17
3.1	Mission statement	17
3.2	Identification.....	17
3.3	Threat perception.....	19
3.4	Vision	21
3.5	Communication	27
3.6	Radio Propagation	27
3.7	Future Work.....	29
4	Physiology.....	30
4.1	Thermal System.....	30
4.2	Metabolic System	35
4.3	Sleep deprivation	46
4.4	Future Work.....	47
5	Weapon effects	49
5.1	Weaponry models	49
5.2	Ballistic protection.....	50
5.3	Weapon Effects.....	51
5.4	Future Work.....	55
6	References	56
7	Signature	59

1 Introduction

SCOPE is short for Soldier Capability Optimization for Projected Efficacy and aims at modelling dismounted soldier operations. SCOPE is used for research in the field of operational performance. Operational performance depends on many factors, varying from climate and terrain characteristics to group dynamics and equipment. SCOPE contains models and variables representing many of these factors. This report is a status overview of the models and variables that are currently implemented in SCOPE.

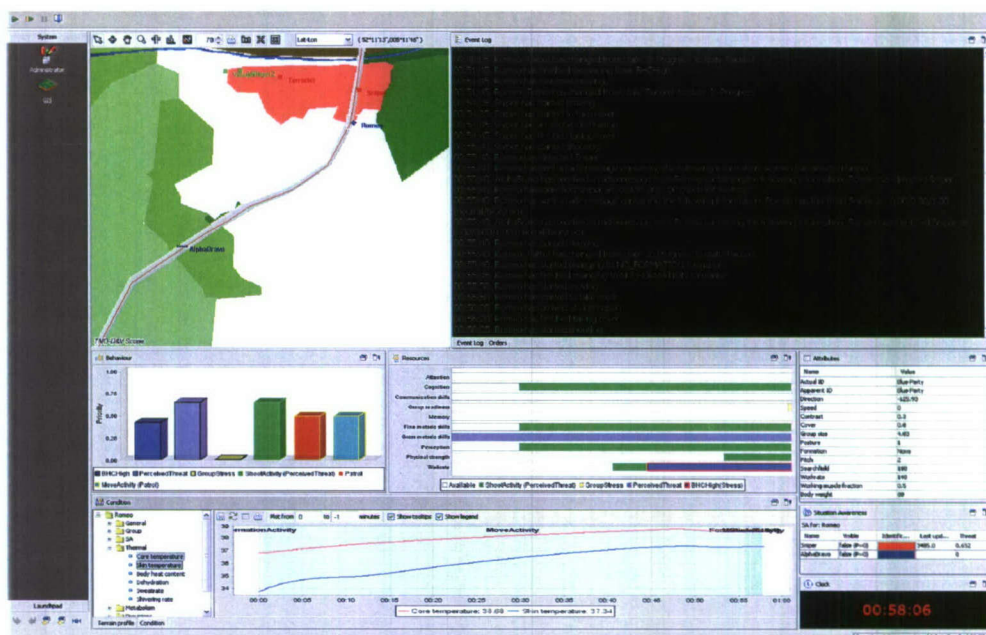


Figure 1 Screenshot of the SCOPE simulation system.

1.1 Overview

In Chapter 2 the SCOPE behaviour model called *CHAOS* is presented. This model is not only used to generate the partly autonomous behaviour of the entities in SCOPE, but is also used to model stress, strain and performance degradation. Besides the SCOPE behaviour model, chapter 2 also contains a description of the model of *group dynamics and readiness*.

In Chapter 3 all models and variables that are related to *situation awareness (SA)* are presented. The subjects range from the technical aspects of perception and communication, that serve as input for SA, to the internal representation of the current situation, i.e. the actual SA. The latter involves for instance the (subjective) identification of people and threat perception.

In Chapter 4 the physiological models in SCOPE used to model physical performance and fatigue and exhaustion are presented, i.e. models of the human metabolic and thermal systems and a model of sleep deprivation.

Finally Chapter 5 deals with the SCOPE models of weaponry, ballistic protection and weapon effects.

2 Behaviour

SCOPE is a research tool aimed at addressing research questions in the field of operational performance. For such a tool a realistic behaviour model is essential since performance is a direct resultant of behaviour. In order to predict operational performance correctly, behaviour will not only have to be influenced by the task or mission at hand but also by situation awareness, group dynamics, clothing and equipment, stress and strain and the environment. This is where the field of human behaviour modelling comes into play.

2.1 Human Behaviour Modelling

In Figure 2 a schematic overview of human behaviour modelling is given. When thinking about behaviour people tend to focus on performing tasks or achieving goals, i.e. in terms of *goal directed* behaviour. However, in reality behaviour is influenced by many more factors. In Figure 2 these factors are grouped together as 'stress'. In this context, stress should be interpreted very broadly, meaning *anything that is conflicting with the goal directed behaviour*.

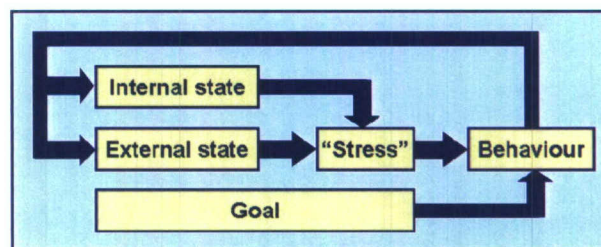


Figure 2 A simple model of behaviour and operational performance.

To give an example: let's assume a postman is delivering mail (goal directed behaviour), when suddenly a big and aggressive dog starts to chase him. This change in the external state will result in a stress reaction (fear), causing the postman to run away from the dog. This will in turn start affecting his internal state: the postman will start to get tired. Now, let's assume that after a while the dog will return home. The postman, still a bit scared, might continue to run for a while, thereby changing the external state (as perceived from the postman's perspective): the distance to the dog will increase. This increase in distance will result in a decrease in fear. After a while the postman will be more exhausted than he is scared, at which point he will start resting. Only when both stressors (fear and exhaustion) have returned to acceptable levels, the postman will resume his goal directed behaviour, i.e. delivering mail.

What this simple example shows is that one of the difficulties in modelling behaviour is dealing with exceptions. The postman simply delivers mail, unless he is chased by a dog. In this case he will run from the dog, *unless* he is too exhausted to run. All these exceptions make it difficult to model behaviour in a centralized way, i.e. by creating a centralized rule base that decides what actions should be taken given the current situation. Such a centralized component would then have to deal with all goal directed behaviours and with all exceptions. However, as the realism of the simulation (and the behaviour model) increases, the list of exceptions will grow, resulting in a model that is difficult to maintain and that is mainly about dealing with exceptions. This puts a severe strain on the modeller as he has to envision all exceptions that might occur beforehand. This of course can be considered a recipe for error.

A better solution might be to model behaviour as a decentralized system consisting of several autonomous components (a multi-agent system). The SCOPE behaviour framework (CHAOS) is such a decentralized system. It is inspired on the pandemonium model of letter recognition as proposed by Selfridge (Selfridge, 1959). Before the CHAOS framework is presented, the following section will provide some background on Selfridge's pandemonium model.

2.2 Pandemonium model of letter recognition

In (Selfridge, 1959), a model of letter recognition is proposed that consists of a collection of simple but autonomous components, called *demons*. Each demon is capable of performing a specialized but simple task. The figure below shows that there are several types of demons. The *data demon* is responsible for representing the letter as presented to the system, to the other demons. To the right of the data demon a layer of *feature demons* is positioned. These demons are capable of recognizing a specific feature. When a feature demon recognizes 'his' feature he will get excited and start to shriek. Next to the feature demons are the *cognitive demons*. These demons are sensitive to a certain set of feature demons. Cognitive demons will shriek louder as more of 'their' feature demons are shrieking. Finally, the *decision demon* decides which cognitive demon is shrieking loudest, i.e. which letter was presented to the system.

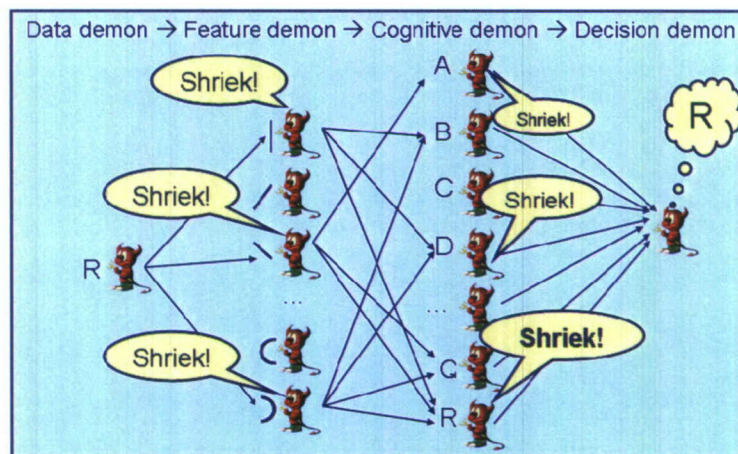


Figure 3 Schematic overview of pandemonium model of letter recognition.

2.3 The CHAOS behaviour framework

CHAOS (Capability-based Human-performance Architecture for Operational Simulations) is the behaviour framework used in SCOPE. CHAOS is loosely based on the pandemonium model just described. The demons in CHAOS however are not capable of recognizing features or letters but should be considered as specific types of behaviour, or *behaviour chunks*. These behaviour chunks are competing for the control of the behaviour of the entity they are part of.

Besides demons CHAOS consists of *resources* and of course of the *pandemonium* itself. The resources represent the *capabilities* of the modelled entity while the pandemonium is the 'arena' in which all takes place and that *controls and coordinates* the whole 'behaviour process'. In order to explain how the CHAOS model works, these three types of components (demons, resources, pandemonium), will be described in more detail in the following sections.

2.3.1 Demons

As stated above, the demons in CHAOS are to be considered as *behaviour chunks*. To better understand what is meant by 'behaviour chunks' it is probably useful to discuss two ways of decomposing an intelligent system into subsystems: the 'normal', or at least, intuitive way and the decomposition as used by the CHAOS framework.

2.3.1.1 Functional decomposition

An example of a simple but typical scheme for decomposing an intelligent system into subsystems is given in Figure 4. This is a decomposition along the functional lines of the subsystems: some part of the system deals with perceiving the world, another part deals with interpreting the things perceived, and finally there is a component that deals with (re-) acting, thereby possibly altering the environment. Let us call this type of decomposition a *functional* decomposition.

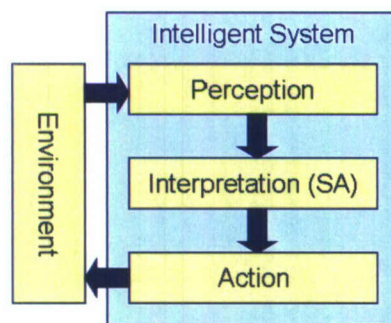


Figure 4 A simple but typical 'functional' decomposition of an intelligent system.

Although a functional decomposition certainly has many useful applications, as a basis for a human behaviour model in a high fidelity constructive simulation it has a major drawback. This drawback has to do with dealing with exceptions and special cases. Let's use our postman example from Section 2.1 again and try to map the above functional decomposition onto the postman's task. The perception layer is responsible for perceiving the outside world (such as mailboxes and dogs). The interpretation part has to do with understanding that the one object is a mailbox, and the other object is a dog. This means that in a behaviour model, this interpretation layer is responsible for recognizing all objects that might be relevant to the postman, i.e. not only objects relevant to the goal directed behaviour, but also to any of the 'exceptional' behaviours. The action layer deals with taking the appropriate action given the current interpretation of the situation. Again, this layer has to deal with both the goal directed and the other, more reactive behaviours. Why this can become problematic when dealing with realistic simulations is explained in the postman example in Section 2.1.

2.3.1.2 Behavioural decomposition

CHAOS uses a different kind of decomposition we could call *behavioural decomposition*. This decomposition is not along the functional lines of the system, but is based on isolated 'chunks of behaviour'. These behaviour chunks are in fact the demons in the pandemonium.

In our postman example a typical demon would be responsible for 'dealing with dogs', while another is responsible for 'delivering mail' (see Figure 5). When we look closer at these demons in Figure 5, it shows that the demons themselves are decomposed functionally. In other words, each demon is responsible for the whole 'behaviour chain', from perception through interpretation to action, but only for a very specific type of behaviour.

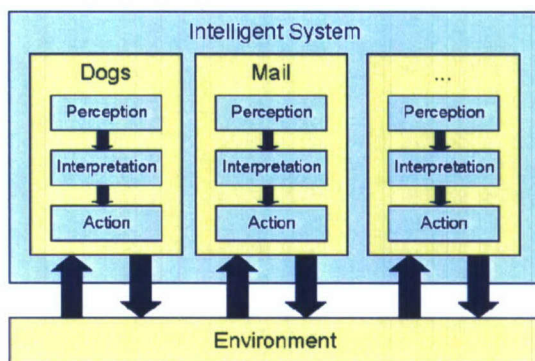


Figure 5 A Behavioural decomposition that might be used in CHAOS to model a postman. One behaviour chunk, or *demon*, is responsible for dealing with angry dogs. Another is responsible for delivering mail. The system will probably contain many more demons, as denoted by the three dots in the rightmost demon.

This is of course just another way of organizing the same behaviours. The behaviour model still has to be able to deal with exceptions, and the modeller still has to envision which types of behaviour may occur. Although this is true, CHAOS has a major advantage over a functionally decomposed system: the behaviour producing components do not have to deal with exceptions themselves. This responsibility is shifted to a higher level structure: the pandemonium. At any given time the pandemonium controls which demons are active. Note however that to do so the pandemonium does not need to understand the behaviours or the current situation. How this is achieved will be explained in Section 2.3.3.

The main advantage of this shift in control is that the demons are truly specialized (see Figure 6). A demon is, in other words, responsible for a specific type of behaviour and is therefore monitoring only that portion of 'the world', i.e. the state space, that is relevant to that type of behaviour. He has to be able to interpret only the situation in this part of the state space, and he has to be able to (re-)act accordingly.

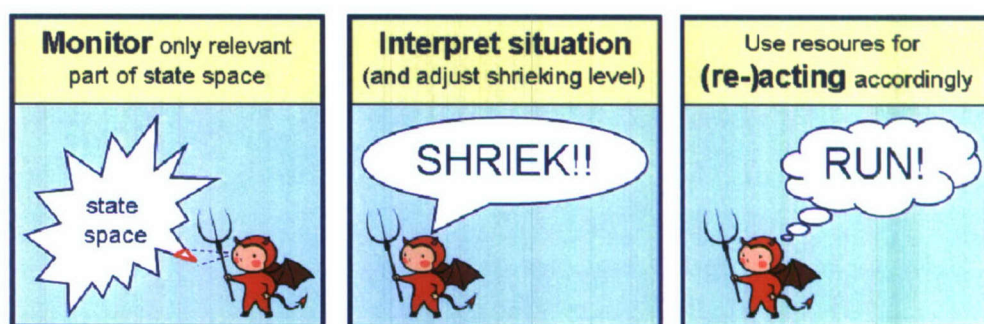


Figure 6 A specialized demon only needs to monitor a small part of the entire state space. He is only able to assess the situation in this small part of the state space, and he can adjust his shrieking level accordingly. He is also able of taking actions if necessary.

From the perspective of the modeller, this specialization means that he can focus on a specific type of behaviour while designing and implementing a demon, without having to deal with exceptions. If the modeller has forgotten to account for a specific type of behaviour (for instance dealing with angry dogs) he does not need to alter any of the existing behaviours but only has to create a new demon that is capable of producing the lacking behaviour.

2.3.1.3 Stress and Strain

Demons are not only used to represent tasks or activities but can also represent stress or strain. Let's say we want to model *thermal stress*, i.e. stress related to the thermal condition of a person. In that case we can implement a 'thermal stress demon' that monitors, for instance, the person's core temperature, and that will shriek louder as the core temperature of that person rises. This demon would then impair some of the capabilities of the system, depending on the demon's shrieking level. How this is achieved will be explained in detail in the following sections.

Note however that besides impairing capabilities a stress demon can also implement a *behavioural* component, just like a 'normal' demon would. In the case of a stress demon this behaviour represents the entity's strategy to *recover or escape from the stressful situation* the entity is in. In case of thermal stress this might involve eating ice cream, taking a swim, or taking a rest from physical activities.

2.3.1.4 Hierarchical behaviour

In the discussion on behavioural decomposition it was proposed that 'delivering mail' is potentially one of the demons in a postman's pandemonium. However, when we look closer at this task it seems to be quite complex, involving many activities ranging from route planning and route following to finding the correct mail boxes and delivering letters to the correct addressees.

If we would model a task of this complexity as a single behaviour chunk the advantages of our behavioural decomposition might be lost. Therefore, in CHAOS behaviour can be structured in a hierarchical way. This means that each demon can have 'child-demons' that might be considered 'sub-contractors' responsible for performing a specific aspect of the more complex behaviour of its parent.

In our postman example, the main parent would be the demon responsible for delivering mail. It may have several child demons, for instance a demon that is capable of planning the route (given the mail that needs to be delivered), another demon that is capable of following the given route, and still another that knows where to interrupt the route following demon to deliver the letters.

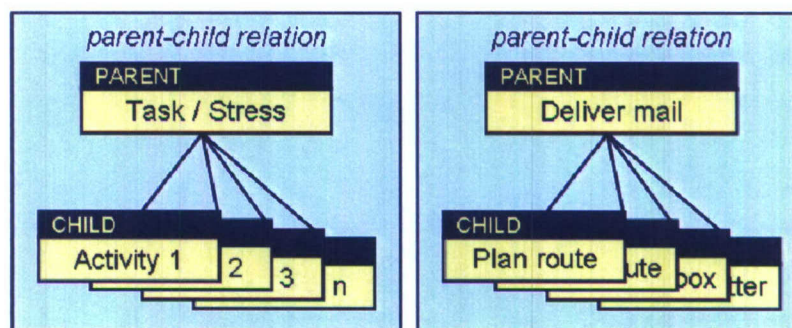


Figure 7 Hierarchical behaviour modelling in CHAOS. On the right a possible implementation of the task of delivering mail.

The interaction between the parent and its children consists of the parent controlling at any point which children are active and which are not. The children in turn inform their parent of their progress. In our example: the parent demon (deliver-mail) knows that the first child that needs to be activated is the route-planner demon. This demon in turn informs the parent when it has finished planning the route. Once the parent demon is informed that a route is calculated, it can de-activate the route-planning demon and activate the route-following demon (and provide the route just calculated), etcetera.

Activating a child demon simply involves changing it's shrieking level. The parent demon would usually activate a child by setting it's shrieking level to it's own shrieking level. Once this is done, the child 'is on it's own' and has to compete with all other demons in the pandemonium. A parent can de-activate child demons by setting their shrieking level to zero. Demons with a shrieking level of zero do not take part in the competition in the pandemonium.

2.3.2 Resources

We saw already in Figure 2 that behaviour is triggered by goals ('Task') or is more reactively triggered by stress or strain ('Stress'). This is again depicted in Figure 8, which also shows the central role *resources* play. These resources are in fact the *capabilities* of the system that is modelled. Such capabilities might be *attention*, *fine motor skills*, or *potential work rate*¹.

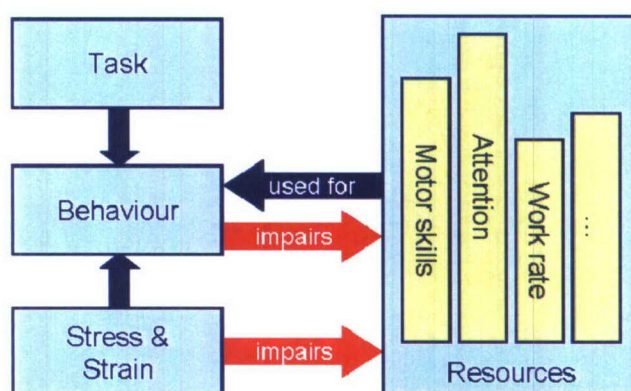


Figure 8 The central role of resources in the modelling of behaviour in CHAOS. Behaviour is determined by stress, strain and/or the execution of tasks. Behaviour can only be executed if the relevant capabilities are sufficiently available. Behaviour and stress can both impair the capabilities of the system.

The demons in CHAOS need to compete over these scarce resources in order to produce behaviour. The more important a demon is (i.e. the louder he shrieks), the bigger the chance is that he will get the resources he needs. Demons can only produce behaviour if the capabilities (resources) needed for their specific type of behaviour are available. This mechanism is represented by the blue arrow in Figure 8.

2.3.2.1 Multi-tasking

In CHAOS, multi-tasking is controlled almost automatically by the fact that two conflicting behaviours are competing over the *same* resource. For instance, if a postman is delivering mail, he probably needs some gross motor skills in order to walk along his route. When he is suddenly being chased by a dog, he also needs these motor skills for running. This of course implies that both activities (walk to deliver mail, run to escape from dog) can not be performed simultaneously, meaning that a choice has to be made. We can also see in Figure 8 that behaviour itself might impair the capabilities of the system (top red arrow). This represents the fact that some behaviours that are not competing over the same resources still can not be performed simultaneously. This is another mechanism used to control multi-tasking.

¹ Which capabilities are actually modelled depends on the behaviour that needs to be modelled, the types of stress and strain that should affect performance and the need for restricting the combination of behaviours ('multi tasking').

For instance, running will *affect* the fine motor skills, even though fine motor skills are not *needed* for running. This is modelled by having any behaviour involving running impair the capability 'fine motor skills'. Any behaviours that depend on this fine motor capability will in turn not be executed or will be executed badly.

Whenever two behaviours can not be executed simultaneously a choice will have to be made. This choice is not made by one of the demons but by the pandemonium.

How this works will be explained in Section 2.3.3.

2.3.2.2 *Stress and strain*

Another important aspect of the role resources play in CHAOS has to do with stress and strain. Stress or strain can not only trigger behaviour but may also directly affect performance. For instance: when a person gets tired while running he may decide to take a rest (stress triggers a change in behaviour) or he may continue running, but will have to lower his speed (stress affects the performance of the active behaviour). This first type of effect is represented by the arrow from 'Stress & Strain' to 'Behaviour' in Figure 8. The second type is represented by the bottom red arrow, where stress directly 'consumes' some of the resources of the system without delivering any behaviour in return.

2.3.3 *Pandemonium*

So far we have covered the resources, or capabilities of the system, and the behaviour chunks called demons that are responsible for behaviour and that can affect the resource levels. However, a demon is not allowed to control the behaviour or influence the resource levels of the entity completely autonomously but it needs 'permission' to do so by the pandemonium. In fact, every demon is part of (contained in) the pandemonium, and the pandemonium controls when demons are updated and which demons get to influence the entity's behaviour and resource levels. The updating process is shown schematically in the flowchart below.

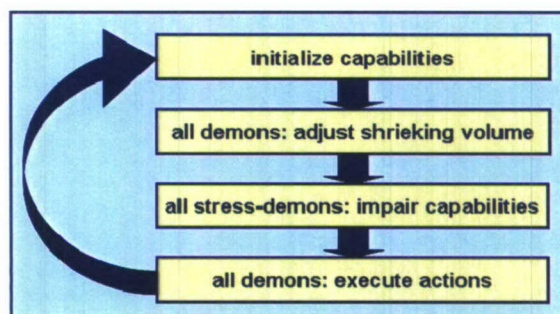


Figure 9 Periodic update of pandemonium. Iterating over demons is done on a sorted list, starting with the loudest shrieking demons.

The above procedure is called on a regular basis. The procedure starts with resetting the resources to their initial levels. After that all demons are ordered to update their 'shrieking levels', given the current state of the simulation. In the next step all demons representing some form of stress or strain are allowed to impair the resource levels. Finally all demons are requested to perform actions, but due to the limited resources only a small amount of demons (possibly just one) will actually take some actions/produce behaviour. In this last step the demon that is shrieking loudest will be the first to be asked to execute his actions. In order to do so, he will probably use some of the resources, leaving less resources for the next demon in line, etcetera.

Figure 10 zooms in on the procedure demons follow to produce behaviour. A demon will start by checking if enough resources are available. If this is not the case it will

return without taking actions or using resources, leaving the turn to the next demon in line. If enough (but possibly less than optimal) resources are available, the demon will take these resources and perform his actions. In case the resource levels were indeed less than optimal, the demon may alter his performance (if this is the case depends on the specific implementation of the demon). This is how for instance stress may lead to a drop in performance (stress-demons take some of the resources before any behaviour is produced. This leads to less-than-optimal resource levels, which might lead to less-than-optimal performance).

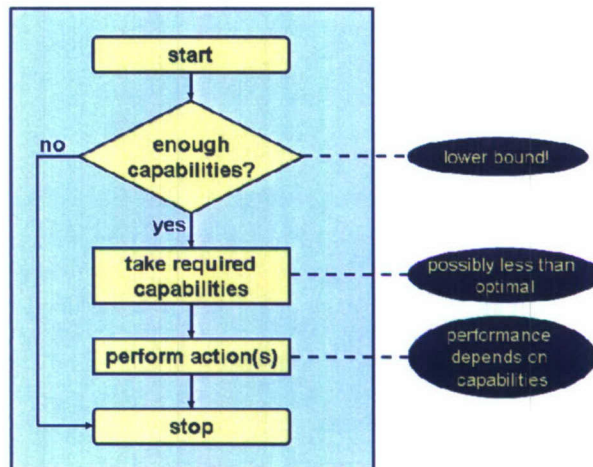


Figure 10: The procedure a demon follows to produce behaviour.

Simply by sorting the demons to their shrieking levels, the pandemonium can – without knowing anything about the specific behaviours or stressors that are active – have control over all the demons it contains. The fact that the demons require and make use of the limited set of resources assures that, if two or more behaviours are conflicting, only the most important one(s) will be performed. Neither the pandemonium or the demons are fully responsible for dealing with exceptions. Still, the system as a whole is capable of controlling when an exception should alter the ‘normal’ (goal directed) behaviour and when it should not. This principle is what makes the CHAOS framework suitable for complex behaviour modelling.

2.4 Group dynamics and readiness

Completely differing from a framework for behaviour modelling, but nevertheless very related to behaviour, is the research on group dynamics. The operational performance of a group of soldiers depends for a large part on the processes and dynamics within the group. In the project ‘Mentale inzetbaarheid’ (‘Mental readiness’) a model of these group processes was created (see for a complete description of the study and results De Bruin, Verwijs & Van Vliet, 2007).

Based on various studies of literature (see for a summary Van Vliet, Van Amelsfoort & Van Bommel, 2004) the variables that are most relevant for mental functioning of an operational unit were identified. Every variable has a direct and/or indirect effect on the team’s operational performance, called ‘team readiness’.

Table 1 The variables used in the group dynamics and readiness model.

Variable	Description
Team age	Since group members get to know each other better and share important events, both group members and the group as a whole change, thereby mainly affecting the cohesion and performance. This is also an indication of the experience of the team.
Leadership	It is assumed that the more leadership styles a leader masters, the more effective his leadership is (see for instance Hersey & Blanchard, 1996). Leadership influences both group members and the group as a whole.
Cohesion	The attractiveness the group has on its members, together with the members' motivation to remain in the group and their resistance to leave the group has a positive relation with the social support the members experience (Rollinson, 2002) and the performance of the group as a whole (Oliver, et al., 1999).
Social support	Through interaction with other group members emotional and practical support is received. This strengthens solidarity and interpersonal relations (Griffith, 1997) and attributes to group performance.
Diversity	Groups are mainly effective if they are diverse in the information and skills the members bring to the group, and at the same time are not diverse when it comes to values (Jehn, Nortcraft & Neale, 1999).

Based on various studies found in the literature, the model shown in Figure 11 was created. The arrows are labelled with an indication of the type of relation connecting the variables.

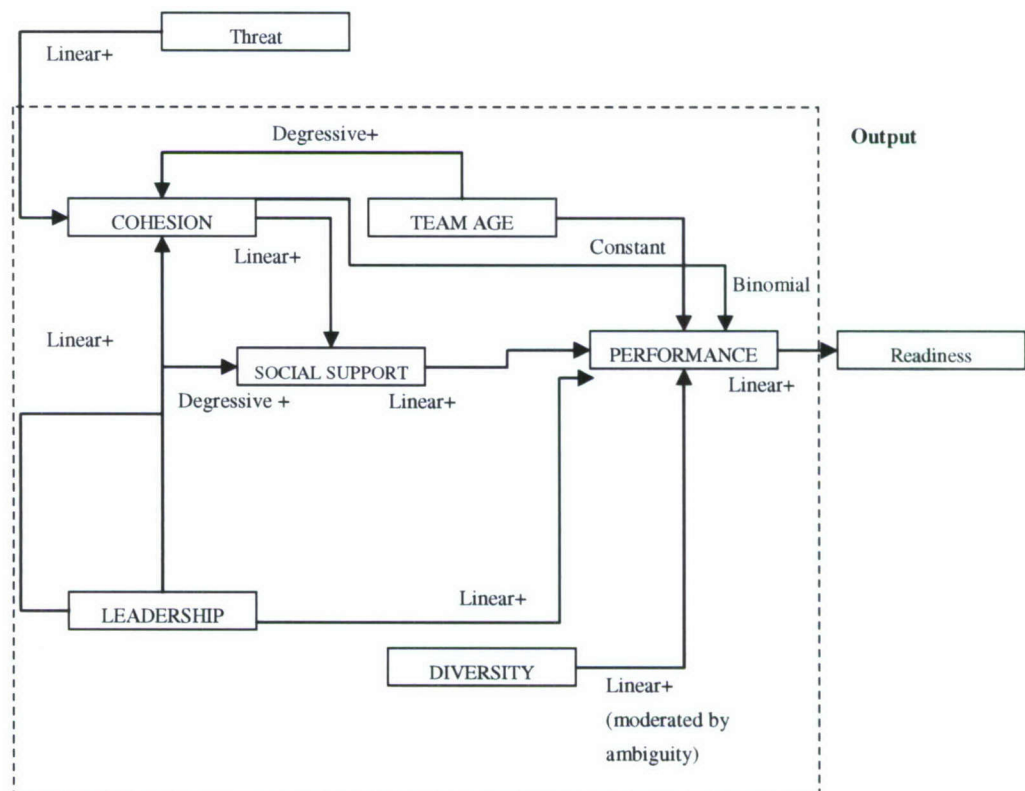


Figure 11 The model of group dynamics and readiness.

2.5 Future Work

The pandemonium behaviour model is a useful framework for modelling behaviour and operational performance. However, it is just a framework and the current version of SCOPE could be improved by making better use of this framework. The modelling of task execution can for instance be improved by making more use of the capabilities and resources needed for and affected by task execution. For instance, cognitive workload is currently not modelled while it is in reality an important factor in operational performance. Another aspect that could be integrated into the pandemonium is visual perception.

The vision model is currently implemented as a 'stand-alone' model that is not integrated within the pandemonium, meaning that the entities in SCOPE are simply continuously perceiving their environment. Visual perception does not require or affect the resources as specified in the pandemonium. The validity of SCOPE could be improved by linking models such as the vision model to the pandemonium.

The same holds for the group dynamics model (see Section 2.4). This model is only linked to the pandemonium through the readiness output variable, which serves as a pandemonium resource. This might be improved by using (some of) the underlying variables, such as diversity and leadership, directly as resources. These new resources could then influence the performance on certain tasks.

3 Situation Awareness

Situation awareness (SA) is an important factor in operational effectiveness. Situation awareness is also a rather vague concept that is hard to model and formalize. SCOPE nevertheless contains several aspects that can be considered as part of or related to SA. In this chapter the most important models and variables related to SA are described, varying from intelligence and threat perception to vision and communication.

3.1 Mission statement

In the current version of SCOPE any pre-mission intelligence is incorporated in the so called *mission statement*. Besides intelligence this mission statement contains information on the active rules of engagement in the scenario. Possible rules of engagement are:

- Do not shoot.
- Shoot when fired at.
- Shoot when in sight.

These rules of engagement are specified for every combination of entities (for instance, the default rule of engagement for a blue entity that encounters another blue entity will be 'do not shoot'²).

The intelligence part contains the following information:

- Default threat: this is a slowly decaying factor that is used in the threat perception module described below.
- Assumed firearms and grenades for every entity type (i.e. red, green and blue entities): again used by the threat perception model. This information is needed to assess the probable threat as exposed by an entity (see Section 5.3.1).

These assumptions are replaced by the actual weaponry used when fired at.

3.2 Identification

In order to describe the identification process as modelled in SCOPE we will call the entity that is identifying the 'entity' and the entity that is being identified the 'target'. The complete identification process in SCOPE is shown in Figure 12. Targets are identified probabilistically; a target can for instance be identified as 'probably red, but possibly blue'. The identification is represented as the three probabilities $p(ID=green)$ (the probability that the target is a neutral entity), $p(ID=red)$ (enemy force) and $p(ID=blue)$ (own/friendly force).

The identification process starts with visual identification. With visual identification it is possible to determine the so called 'Apparent ID' of an entity, i.e. to determine what an entity *looks like*. Whether visual identification is successful depends on the contrast as calculated by the vision model (see Section 3.4).

If visual identification fails the target will remain unidentified, unless it has been seen shooting at the entity, in which case it will be identified by the entity as hostile. If visual identification is successful then military targets (i.e. targets who's apparent ID is 'red' or 'blue') will be classified accordingly whereas the classification of entities that appear to be neutral depends on the amount of 'distrust', a concept that will be clarified in Section 3.3.

² Note that this does not per se prevent blue-on-blue engagements since this is caused by misidentification resulting in the wrong rule of engagement being applied.

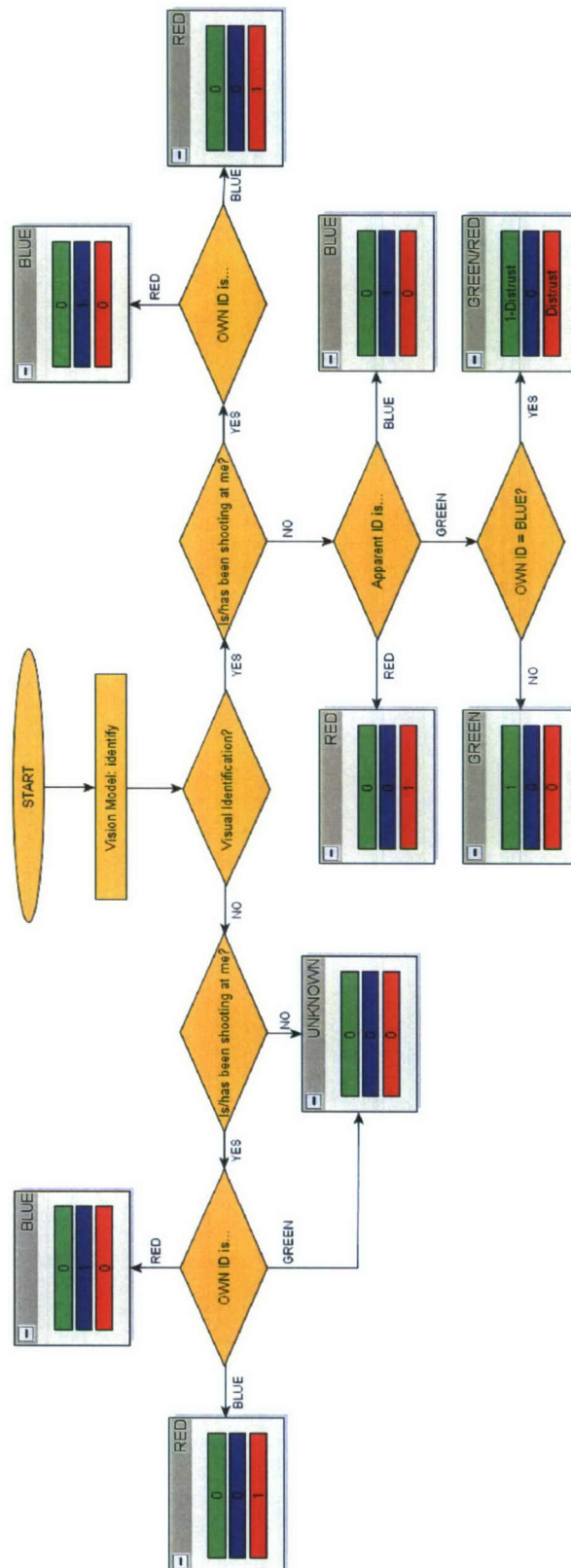


Figure 12 Identification process as implemented in SCOPE. Note that in SCOPE entities have an apparent ID ('what they look like') and an actual ID ('what they are'). The boxes with the three colored bars represent the (assumed) probabilities of the identified entity belonging to the blue, red or green forces. Note that in the identification of green/red entities, the entity's ambiguity is also taken into account (see Section 3.3.1).

3.3 Threat perception

An important aspect of the SA model in SCOPE is concerned with threat and threat perception. Threat perception is closely linked to the identification process since the identity of entities is important in determining the threat as exposed by these entities. The threat perception scheme and the interrelatedness with the identification of entities are shown in Figure 13. The main variables in the threat perception scheme are *distrust*, *subjectively* and *objectively perceived threat* and *perceived threat*.

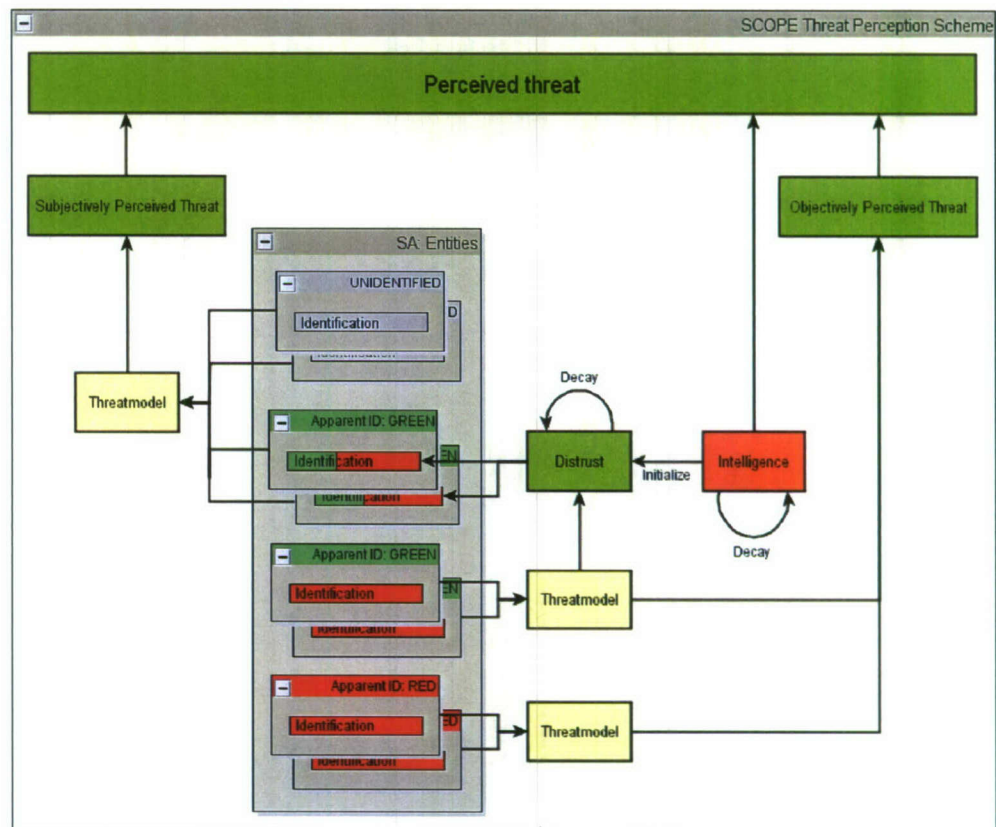


Figure 13 The threat perception model in SCOPE, from the perspective of a blue entity (green entities are neutral, red entities are hostile/enemy force). Threat perception is closely linked with the (assumed) identity of the entities that are represented in the SA component. The representations of the entities in the SA component have an 'Apparent ID' (i.e. 'what they look like') and an identification (i.e. 'what the entity the SA belongs to thinks they are').

3.3.1 Distrust

Distrust is a measure for the lack of trust entities have in *apparently neutral* entities. The initial level of distrust is given as part of the intelligence provided in the scenario. During the simulation distrust can increase as apparently neutral entities are identified as hostile, i.e. as 'terrorists'. The threat exposed by these terrorist entities, as calculated by the threat model (see Section 5.3.1), can only increase and not decrease distrust, as can be seen from Figure 14. When the exposed threat by terrorist entities is lower than the current distrust, distrust will slowly decay ('no news = good news'). When distrust is high, apparently neutral entities will be perceived as threatening, i.e. $p(ID=red)$ rises with distrust (see Figure 12 and Figure 14). To determine this assumed probability of an entity belonging to the red force, the ambiguity of that entity, a property that is given in the description of the entity in the scenario, is also taken into account.

Ambiguity can range from 0 to 1 and is used to represent the fact that the identification of for instance a group of young men will usually be more sensitive to distrust than the identification of a group of children. This is accomplished by setting the ambiguity of the young men to a high value and the ambiguity of the children to a low value. The actual distrust (i.e. $p(ID=red)$) for a given entity i is then calculated as follows:

$$p(ID_i = red) = ambiguity_i \cdot distrust$$

Equation 1 Calculation of probability that the ID of entity i is red.

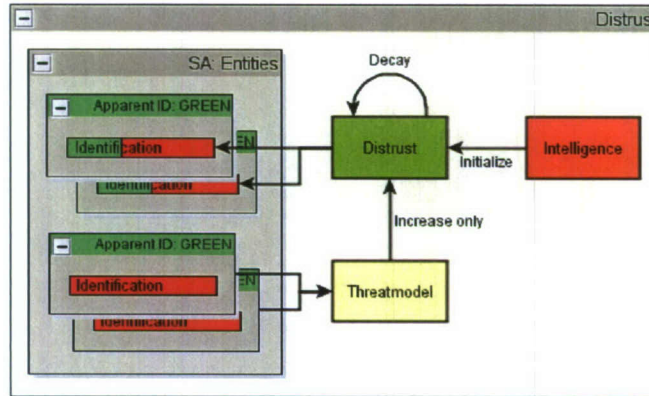


Figure 14 The role of distrust within the threat perception scheme. Note that the influence of ambiguity is not shown in this figure.

3.3.2 Subjectively and objectively perceived threat

Subjectively perceived threat represents the threat as exposed by entities that are not (yet) identified as hostile, i.e. neutral entities and unidentified entities (see Figure 15). The formal definition of subjectively perceived threat is given in Equation 2.

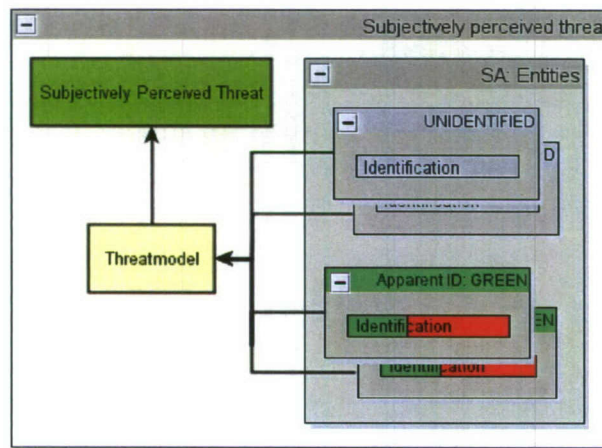


Figure 15 Subjectively perceived threat.

$$T_{subjective} = \sum_{i \in U} threat(i) \cdot distrust + \sum_{j \in G} threat(j) \cdot p(ID_j = red)$$

Equation 2 Calculation of subjectively perceived threat. U represents the collection of unidentified entities, G represents all entities that appear to be green. $threat(i)$ is the threat exposed by entity i as predicted by the threat model (see Section 5.3.1).

Objectively perceived threat is complementary to subjectively perceived threat and represents, from a blue perspective, the threat exposed by all entities that are identified as red entities (see Figure 16). Objectively perceived threat is calculated as follows:

$$T_{objective} = \sum_{i \in R} threat(i)$$

Equation 3 Calculation of objectively perceived threat. R represents the collection of entities that have been identified as red. $threat(i)$ is the threat exposed by entity i as predicted by the threat model.

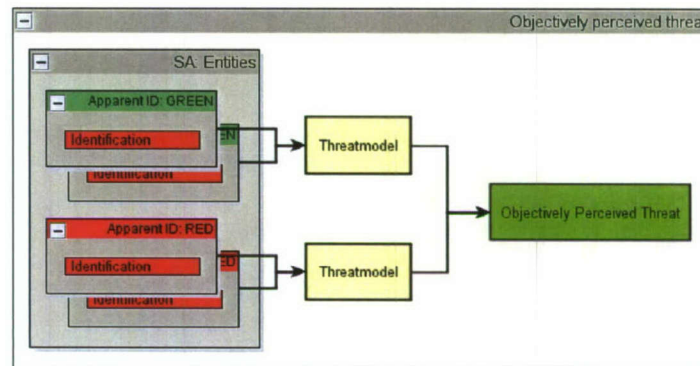


Figure 16 Objectively perceived threat.

The total perceived threat is then simply calculated by taking the maximum of the default threat as given as intelligence, and the sum of the subjectively and objectively perceived threat (see Figure 17). Note that the influence of intelligence will decay, thereby representing the fact that assumptions made beforehand are replaced by information gathered during the mission.

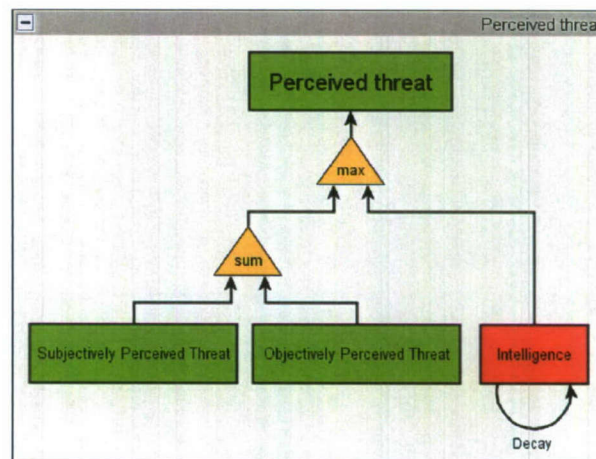


Figure 17 Total perceived threat.

3.4 Vision

Extensive studies have been done on the detection of targets in a visual scene. The discrimination and recognition process involved is highly complicated. Numerous image characteristics have been studied in relationship with the sensitivity of the eye for it, such as spatial frequency, contrast, image features, attention, colour

discrimination, motion perception, disparity and many other. Vision is hardly separable from cognition. The eye does not see, the brain does. What the eye sees lacks meaning and the reference model (template of what is being looked for), stored in an abstract way in memory, is used to set the search cues. Also motor action is involved as searching a scene follows a strategy, the fixations of the eye jumping from one place to another. Depending on the search strategy search time may differ. On the way dynamic processes enhance or suppress the perceived cues.

Models that predict detection and recognition based on psychophysical and psychological knowledge are highly elaborate. Every entity is looking continuously around and the computing power needed to use such models is phenomenal. What we need is a much simpler way to get about the same result. We exploit the concept of conspicuity (Engel, 1977), defined as the angle that the eye may look away from a target before it disappears in the peripheral visual noise. Small targets, similar to the background, static and with modest depth difference have a small conspicuity. Conspicuity is thus a property of an object, compared to its background. Experimental data show that conspicuity and search time are tightly related (Hogervorst et al, 2005). As search time (or detection chance) is what we are looking for, conspicuity is a useful concept to simplify visual detection.

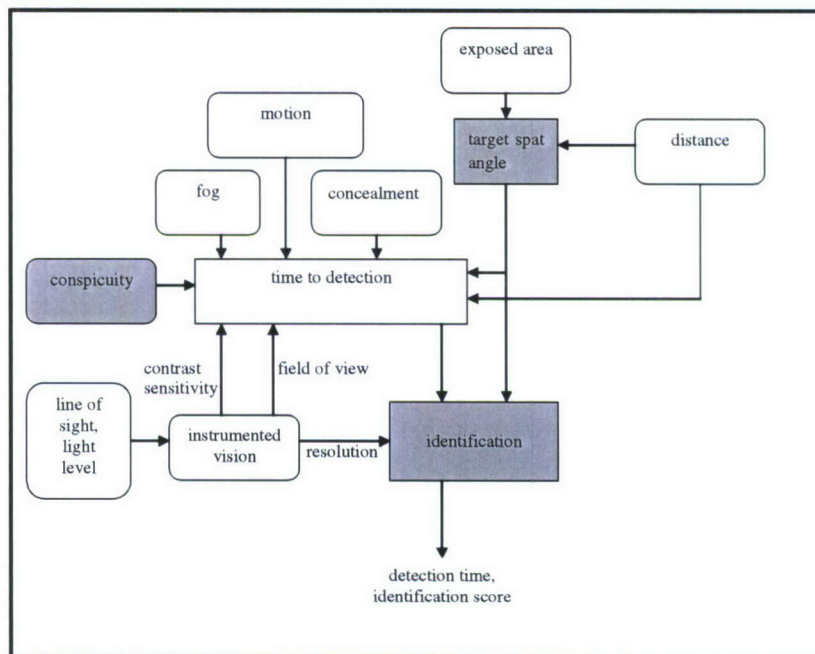


Figure 18 Schematic overview of the SCOPE vision model. Calculations in the shaded boxes are in angles.

A schematic overview of the SCOPE vision model is given in Figure 18. Vision starts with the standardised conspicuity (sometimes referred to as saliency) of targets (during daytime, with naked eye, at a reference spatial angle). Target size (i.e. group size and formation) and distance determine the actual size (in spatial angle) and modify conspicuity. Fog and concealment further reduce conspicuity and motion increases conspicuity, depending on the range.

Detection is a probabilistic process, comparing the observed space to the conspicuity angle and determining the typical time to detection. Vision can be enhanced using magnifying glasses, image intensifiers and thermal imagers. For each of these instruments, field of view and resolution are specified. Target spatial angle is compared to resolution to decide on identification.

3.4.1 Conspicuity

Conspicuity is defined as the angle that the eye may look away from a target before it disappears in the peripheral visual noise. Targets that stand out have a higher conspicuity than assimilated targets. The measure for standing out is an aggregation of luminance contrast, colour contrast, shape (texture and gestalt), depth and motion. Nothdurft (2000) concluded from a study on combined features of targets that luminance contrast, motion and orientation/color, are almost independent, but that even the most independent features do not fully add in saliency strength. Itti et al (1998) stated a model for dynamic attention and eye movements, based on the behavior and the neuronal architecture of the early primate visual system. The model calculates saliency of all objects in a visual field. A dynamical neural network then selects attended locations in order of decreasing saliency. In 1999 Itti and Koch experimentally researched how the local spatial discontinuities in intensity, color, orientation or optical flow, and are combined into a unique saliency. Four combination strategies were compared:

- 1 Simple normalized summation.
- 2 Linear combination with learned weights.
- 3 Global non-linear normalization followed by summation.
- 4 Local non-linear competition between salient locations.

Combination 2 gave best performance for a closed set of pictures, but 3 and 4, which are fairly similar, gave best general results. They can be described as winner takes all. We believe that interpreting conspicuity as a vector length in 5 space delivers nearly the required characteristics, assuming weight factors for the various dimensions.

The difference between unstructured attention and search for military targets leads to slightly different relevant features: luminance, colour and motion are common, object orientation is replaced with pattern difference and depth (assuming that military know what they are looking for), and flicker becomes irrelevant. Thus:

$$\text{conspic} = \sqrt{(C_{\text{lum}}^2 + C_{\text{clr}}^2 + C_{\text{shp}}^2 + C_{\text{dpth}}^2 + C_{\text{mtn}}^2)}$$

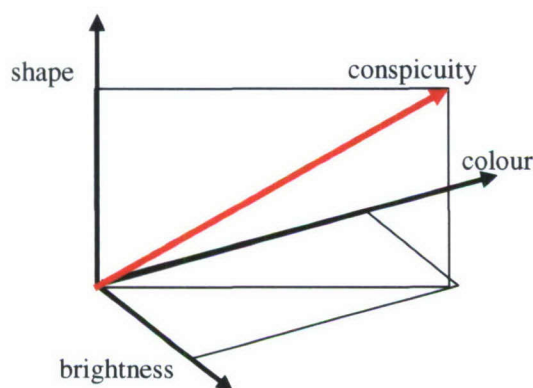


Figure 19 Independent contributions add to conspicuity (only three shown here). When two out of three are cancelled, conspicuity may drop, but not below the remaining contribution.

These are independent inputs and the conspicuity is the vector length in 5 space. Effects such as haze may bleach colour and diminish brightness contrast, but it would hardly affect shape. Since the same happens to the background noise haze does not decrease conspicuity until the target disappears completely. Similar reasoning hold for dimming light. Obviously, this is only approximate, but it allows us to simplify visual detection. We make no further distinction than between day and night, and between within or without visual range.

Standardized conspicuity (in m) is given as a property in the description of an entity in the scenario and converted to the actual distance at which it is observed:

$$\text{Conspicuity} = \text{Conspic}_{st} / d$$

Conspicuity is thus expressed in m/m, which is the tangent of the angle (observed with the conspicuity meter), for small angles equal to the angle itself. Standard conspicuity is dependent on the size of the entity or object. A large object which is equally well camouflaged as a smaller object, is still more conspicuous. Conspicuity suffers from concealment by leaves, branches and other occluding objects:

$$\text{Conspicuity} = \text{Conspic}_{st} \cdot d^{-1} \cdot e^{-d \cdot \text{concealment}}$$

where concealment is the density of occluding objects (in m⁻¹). Motion is counteracting the concealment, because the gestalt is restored, regardless of the missing parts. For practical purposes, motion of the target reduces the exponent to 0 and doubles the conspicuity.

3.4.2 Fog and haze

The visual range of an entity is calculated by taking the light of target and background, weakening it by absorption of the emitted light and masking it by stray light. The original contrast:

$$C_o = (L_o - L_b) / L_b,$$

is turned into

$$C' = C_o \cdot r_b / (r_b + 2 \cdot (l - \tau) / \tau),$$

where τ is the damping factor ($= e \exp(-3d/V_m)$, with d for distance and V_m for meteorological sight) and r_b is the reflection of the background, assumed to be 0.5. When C' drops below 0.05, no contrast is detected and the visual range is reached. Solving C' for d reveals:

$$d = -V_m \cdot \ln(0.2 / (C_o + 0.15)) / 3,$$

suggesting that low contrast objects disappear in the fog immediately, whereas high contrast objects (men in white or black suits) are visible up to 80% of V_m and lights beyond V_m . If the contrast differs from the sensitivity of 0.05 pertaining to the naked eye, namely $k \cdot 0.05$, then in the last formula C_o has to be replaced by C_o/k . Note that even in the absence of fog low contrast objects are invisible.

3.4.3 Search time

The chance of detection depends on the search time (ST), i.e. the time it takes to detect an object. If the search time exceeds 100 sec, the target will not be found. For an object with a given conspicuity the search time is given by:

$$ST = 0.1 \cdot \text{searchfield} \cdot \text{conspic}^{-2/3}$$

To determine the chance on detection, we calculate the probability that a target is detected in the first second, the second, the third, etcetera:

$$\begin{aligned}
 & p \\
 & p \cdot (1 - p) \\
 & p \cdot (1 - p)^2 \\
 & \dots \\
 & \frac{p \cdot (1 - p)^n}{p(n)}
 \end{aligned}$$

ST is reached at $P = 0.5$. The sum of the series is approximately:

$$P(ST) \approx p \cdot (ST - p \cdot ST \cdot (ST - 1) / 2) \approx 0.5$$

The solution to this equation is:

$$p = (ST - \sqrt{ST}) / (ST \cdot (ST - 1))$$

The series above represents the increase of P over time.

3.4.4 Detection time

Detection remains a probabilistic concept. When an entity approaches, p increases as the distance gets shorter and depends on the time: $p(n)$. The total chance on detection is:

$$P(N) = \sum_{n=1}^N p(n) \cdot (1 - p(n))^{n-1}$$

Again the average detection time ST is reached if $P(ST) = 0.5$.

3.4.5 Groups

We assume that groups are so efficient as to share what has been detected and to search the search area in a coordinated way. When two groups are approaching, the chance of group 1 to detect an individual of group 2 is magnified by the size of group 2 (more targets) and by the size of group 1 (more eyes sharing the search area).

$$P_{gr} = p \cdot n_1 \cdot n_2$$

As the detection of one individual narrows the search area, the remaining group members will be detected rapidly after the first.

3.4.6 Visual engagement

If two entities approach, they have the chances p_1 and p_2 to detect each other. Both depend on the distance and thus are changing as they approach. The question here is what the chances are for the parties to see the other party first. How long this takes is of secondary importance. However, the time needs to be set, because the chances for the parties keep changing, converging to unity for both. Waiting too long is thus bad policy.

We calculate the chance that neither party sees the other and watch it drop to 0.5, indicating the average combined detection time. Thus $(1 - P_1) \cdot (1 - P_2) = 0.5$ is the criterion

for detection and $P1/(P1+P2)$ the chance of party 1 to detect first and $P2/(P1+P2)$ for the other party. Who sees first has the advantage of surprise. From this moment on the search field may be narrowed, optimising detection, while staying more hidden. We will assume here that if a group member is detected, the other group members are seen as well, as far as visible at all, while the detecting party stays undetected, until they take action and apply power. From that moment on every member of both entities is detected. The party who detects first may want to move closer before taking action. They will only do so when the risk of being detected is low enough not to give away the advantage. They may steadily increase their threat until a first strike is likely to incapacitate some of their opponents. The expectancy of this event is $\text{threat}_1 \cdot 1$ (the detection took place and the chance on detection is thus unity). For the opponent the expectancy is $\text{threat}_2 \cdot 0$ (at this point in time no detection took place). The strategy is to optimize the own expectancy without letting the opposite expectancy become significant. The starting condition for party 1 is thus that $\text{expectancy}_1 \sim 1$ and $\text{expectancy}_2 \ll \text{expectancy}_1$. In this manner a visual engagement runs into a physical engagement. Taking this a step further, the visual engagement is preliminary to the physical engagement in the chance tree of the engagement. The following example illustrates this:

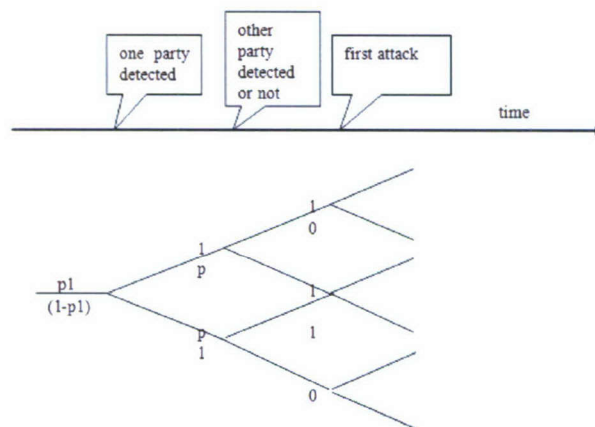


Figure 20 The chances to see the other party vary with time. The party who sees first has the tactical advantage to wait for the optimal conditions to attack. He is taking chances, though. This game may result in either of three starting conditions for the physical engagement.

At the time of detection (first event) the chances are varying in the ratio $p1/(1-p1)$. After detection the chances are conditional. There is the chance $p1$ that party 1 will detect first. The follow up has the conditional detection chance of 1 for party 1 and 0 for party 2. If party 1 decides to wait in order to increase its threat (by coming closer), the detection chance for party 2 increases to p as time proceeds. If party 1 waits too long, his advantage may get lost because party 2 sees him (when $p=.5$). That would be the second event, turning the visual chances in 1 to 1. Until then, the chances are 1 to 0. In either of the three resulting conditions (1/0, 1/1, 0/1) a physical engagement may have distinct outcomes.

3.4.7 Identification

Experimental data show that if an object is found, identification follows very quickly or not at all. Experimental data also show that for those targets that are identified, the mean search-and-identification-time is less than the average detection time. The two are not in contradiction. We assume here that the detection time is equal to identification time and that identification depends on the resolution. For identification the target diameter must be 20 times the resolution, putting a limit to the distance.

3.4.8 Instrumented vision

With a thermal imager, detection is easy, but identification difficult. With an image intensifier detection is similar to with the naked eye (although there is less contrast, resulting in dark shadows) and identification is relatively easy. The contrast range of a thermal imager is less than the eye, resulting in unresolved shaded or bleached areas. However, the thermal imager increases the conspicuity of warm objects and thus works as a magnifier for conspicuity by increasing the contrast of the target. For a part, TI and I2 are complementary. We assume the following:

Table 2 Properties of the various vision devices, including the naked eye.

<i>device</i>	<i>resolution</i>	<i>identification at (m)</i>	<i>contrast sensitivity</i>	<i>fog sensitive</i>	<i>field of view (degr)</i>
1 = naked eye	1 arcmin	350·ε	0.05	yes	up to 180
2 = magnifying optic (magnification m)	1/m arcmin	350·ε·m	0.05	yes	50/m
3 = thermal	3 arcmin	100·ε	0.005	little	20
4 = I2	1.5 arcmin	200·ε	0.5	yes	50

Head movements compensate for narrow field of view. That is not a reason for missing a target. The limitation is that a conspicuity larger than the field of view is not detectable. Instrumented vision thus puts a limit to conspicuity of objects.

3.4.9 Strategy for detection and identification

If an entity has several visual instruments at its disposal we need to stipulate a strategy to use its means. This depends on day/night conditions. During daytime the naked eye, magnifying optics and thermal imagers may be useful. During the night the night vision options are I2 and TI instruments. Twilight is not considered. Weather conditions (fog, dust) may favour TI. We thus need to test all instruments to see what is the best. For identification we do the same. If identification does not succeed, we need to come closer until it does, or apply power anyway, depending on the RoE.

3.5 Communication

Two types of communication events can be distinguished: intra-entity communication (communication within the group) and inter-entity communication (communication between groups). At this moment intra-entity communication is not modelled or is modelled as being perfect, i.e. all information is immediately shared with all group members. Because a group of soldiers is the lowest simulation unit, there is only one SA model maintained for all members in the group and therefore it is not possible to model intra-entity communication correctly.

For inter-entity communication entities use their radios. Whether communication between two entities is possible is determined by the radio propagation model that is described in Section 3.6. Currently, the entities send each other information when an unknown entity has been detected or when a previously detected entity has been identified (or his identification has changed).

3.6 Radio Propagation

The communication devices in SCOPE are described by the attributes listed in Table 3. Given these attributes and some general terrain properties a relatively simple radio propagation model is used to predict if communication between two entities over the

radio is possible. The model also supports radios with relay functionality to enable simulation of ad hoc radio networks.

Table 3 Attributes used in SCOPE to represent communication devices.

Attribute	Unit
Frequency	MHz
Transmit power	dBm
Relay	true/false
Gain	dB
Sensitivity	dBm
Antenna height	m

The propagation algorithm is as follows:

- 1 Calculate the propagation loss (see Section 3.6.1)
- 2 Calculate the system budget P_s
 $P_s = Gain_{transmitter} + propagation\ loss + Gain_{receiver}$
- 3 Communication will be possible if:
 $transmitPower_{transmitter} - sensitivity_{receiver} - P_s > 0$

3.6.1 Propagation loss calculation

To calculate the propagation losses two models are used. If the frequency of the used radio is higher than 1500 MHz the Okumura-Hata model is used (Okumura et al, 1968) otherwise the COST 231 extended Hata model is used (EUR 18957, 1999).

In case of rural terrains a terrain damping factor (TDF) that is given as an attribute of the terrain types, multiplied by the distance the signal has to travel, is added to the calculated loss; i.e.: $prop. loss = prop. loss + TDF \cdot distance$.

In the current implementation diffraction due to hills and mountains is not modelled. The following model could be used however to account for diffraction effects (L_d):

$$L_d = \begin{cases} 6 + 9v - 1.27v^2 & 0 < v < 2.4 \\ 13 + 20\log v & v > 2.4 \end{cases}$$

$$v = h_m \sqrt{\frac{2}{\lambda} \left(\frac{1}{d_t} + \frac{1}{d_r} \right)}$$

With:

h_m : height of highest obstacle.

d_t : distance from transmitter to highest obstacle.

d_r : distance from receiver to highest obstacle.

3.7 Future Work

3.7.1 *Vision*

Currently, we work with the unrealistic situation that a target has a fixed conspicuity, independent of the environment it moves in. As shown in Section 3.4.1, a target has visual characteristics that contrast with the environment, as specified per terrain sector. His conspicuity may thus change as he moves into the next sector. We will implement the dynamic conspicuity when we have the right weight factors and threshold values of the components that constitute conspicuity. A further advantage would be that the effect of visibility (smoke and haze) on the visual perception can be based on all components, rather than on luminance contrast alone.

Furthermore, as already mentioned in Section 2.5, SCOPE could be improved by embedding the vision model into the pandemonium model in such a way that the vision model affects and is affected by the pandemonium resource levels. Vision is currently implemented as a 'stand-alone' model that is not integrated within the pandemonium, meaning that the entities in SCOPE are simply continuously perceiving their environment.

3.7.2 *Communication*

As noted above intra-entity communication is missing from SCOPE and would be hard to implement since all group members share a single SA model. In SCOPE 'real' communication between group members would therefore be of no use since all new information is shared with all members immediately anyway. A possible solution for this problem would be to model intra-entity communication in an abstract matter, for instance as a resource in the pandemonium. The level of this resource could depend on group characteristics and equipment. This resource could then influence task performance directly.

3.7.3 *Radio Propagation*

The radio propagation model could be improved by modelling diffraction, as mentioned in Section 3.6.

3.7.4 *Hearing*

Currently missing from SCOPE is an auditive model to model perception through hearing. This model could influence both inter- and intra-entity communication, and could also influence the detection of entities through audio events, such as gun firing. At this moment, gun-firing can lead to detection, but an auditive perceptual model is missing.

3.7.5 *Netcentric warfare*

Modern SA is of course related to netcentric warfare and digital information systems. These aspects are not yet incorporated in SCOPE. Implementing for instance an equivalent of a 'digital soldier assistant' would be very interesting. Modelling the technical aspects of these innovations is not so difficult, modelling the way this would influence decision making and operational behaviour is. This is therefore one of the important challenges ahead for the development of SCOPE.

4 Physiology

4.1 Thermal System

4.1.1 *A constructive thermal simulation model*

The thermal condition of the human entities is monitored by keeping track of heat gain and loss. The heat gain results from physical work and environmental heat (hot air and solar radiation). The heat loss results from convection of heat as warm air, radiation of the body or sweat evaporation. Since the heat loss depends on the physiological reaction, the clothing ensemble and the climatic conditions, quite some parameters are involved: four for climate (temperature, humidity, windspeed and radiation intensity), three for clothing (insulation, vapour diffusion resistance and solar absorption) and three for the body (work rate, weight and stature). The net heat gain is calculated by means of the heat balance equation, resulting in heat storage in the body. A physiological model calculates the physiological reaction and body temperature and dehydration are used as the variables to monitor over time.

The body is in a dynamic thermal state, balancing heat production with heat loss. The balance may involve actively increased or reduced heat loss, controlled by the thermal state. Metabolic heat production is the result of Work rate x time, under subtraction of performed external work. For military tasks external work is often negligible. Work rate includes shivering. Shivering is automatically induced if the appropriate thermal conditions are reached.

Average skin temperature and core temperature are calculated. The skin temperature stands for the body shell and core temperature for the body core, implying that the body is divided into two compartments. For many conditions, in particular in the heat, this is a sufficient distinction. This approach is less suitable for cold stress, because frost bite is a local phenomenon and just two compartments provide insufficient detail. Core and shell are not split in fixed proportions. Rather, the shell is thick in the cold and thin in the heat, due to changes in the blood flow. A simple physiological controller tells the reaction of the body on the thermal conditions. The controller, taken from Gagge et al (1971) and tuned by Havenith (1997), keeps track of internal stimuli, stemming from core and skin, and generates the shivering, blood flow (heat transport) and sweat response. These are used as inputs for the heat balance calculation. Acclimatization and fitness effects on sweating and blood flow are taken into account according to Havenith (1997).

The heat balance equation is calculated at the clothing level, which is the interface with the environment. The clothing ensemble is represented as a single layer, covered with the adjacent air layer. This allows us to include thermal and vapour resistance of the ensemble and to include solar radiation. The combined physiological and clothing model is a simplified version of the model described and validated by Lotens (1993). It does not include ventilation or moisture management inside the clothing, nor does it take account of the fraction of the body covered with clothing. The clothing parameters need to be specified in a knowledgeable way.

Performance is affected by a couple of criteria, that are monitored. Body core temperature is a criterion, but the total heat stored in the body (Body Heat Content or BHC) indicates the general taxing by heat (BHC positive) and cold (BHC negative), including core and

skin. Cold may hamper motor tasks. A low skin temperature is the forecast for low local temperatures. Another performance indicator is dehydration, caused by sweating, depleting the circulating fluid. Water must be taken in to compensate for sweat loss. If not, dehydration of more than 2% of body weight starts affecting the maximal work rate and at 10% drinking cannot restore the water balance any more. Injection of physiological fluid becomes a life saver. Dehydration increases core temperature rise, thus aggravating the thermal condition. Fluid replenishment is limited to 1 l/hr, because absorption in the intestines does not go any faster.

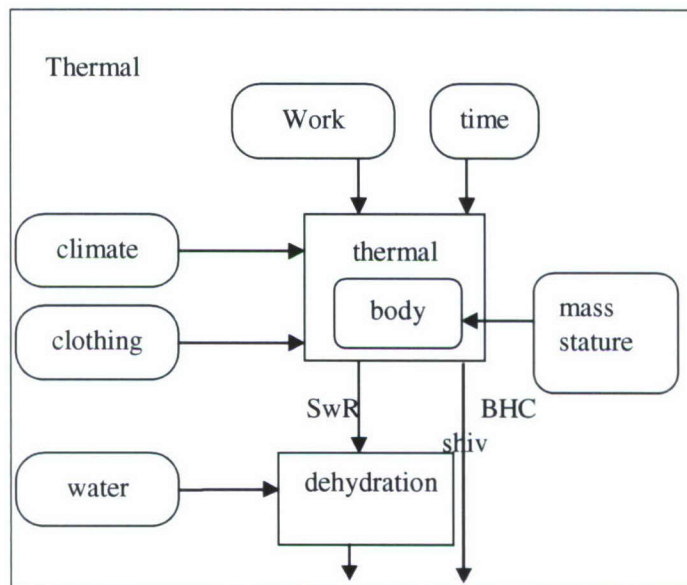


Figure 21 Climate, clothing and work rate determine the heat balance. The thermal condition of the body develops over time and continuous sweating leads to dehydration, unless replenished. Dehydration and thermal overload are show stoppers, shivering hampers fine motor control.

4.1.2 Algorithm

The variables concerned and the calculations are explained stepwise. The outputs are being updated in time steps dt (s). Two differential equations are involved, for body core and shell, respectively.

4.1.2.1 Variables and constants

The following tables contain the input variables (Table 4), calculated variables (Table 5) and constants (Table 6) as used by the algorithm.

Table 4 Input variables.

Category	Variable	Unit	Description
Work	WR	W	Metabolic Rate
	Fit	No dimension	Fitness ranging from 0 to 1. See Section 4.2.2.5
	Acc	days	Nr. of days acclimatized
Climate	Ta	°C	Air temperature
	rh	%	Relative humidity
	v	m/s	Air velocity
	sun	W/m ²	Solar intensity
Clothing	dcl	m	Equivalent water vapour resistance of clothing
	lcl	m ² K/W	Clothing insulation
	Epsilon	no dimension	Clothing radiation absorption

Table 5 Calculated variables.

Category	Variable	Unit	Description
Adjacent Air	da	m	Equivalent water vapour resistance of adjacent air
	la	m ² K/W	Insulation of air layer adjacent to clothing
Physiology	Tc	°C	Core temperature
	Tsk	°C	Skin temperature
	BHC	J/g	Body heat content, relative to neutral
	dehydration	l	Loss of body fluid, relative to neutral

Table 6 Constants.

Category	Variable	Value	Unit	Description
Physical constants	He	2430	J/g	Heat of evaporation of water
	D	25 · 10 ⁻⁶	m ² /s	Diffusion constant of water vapour in air
	lambda	0.026	W/mK	Heat conductivity of air
Body reference values	Tc _{ref}	36.8	°C	Neutral temperature the body strives for
	Tsk _{ref}	33.7	°C	Associated neutral skin temperature
	A	2	m ²	Body ₃ surface area of an average young Dutch male
	W	75	kg	Average body weight for a young Dutch male ⁴
	S	1.83	m	Average stature of a young Dutch male ⁴
	Acclim	1 · 10 ^{-0.3(acc-1)}	nd	Effect of being acclimatized [0..1]

4.1.2.2 Calculations for the physiological control

The following tables contain the calculations for the physiological control.

Table 7 Converting the climate inputs into useful variables.

Var.	Calculation	Unit	Description
Sat	$1000 \cdot e^{(23.56 - 4030/(T+235))} / (461 \cdot (T+273))$	g/m ³ , T in °C	Water vapour saturation concentration at temperature T
Ca	$rv \cdot \text{Sat}(Ta) / 100$	g/m ³	Vapour concentration in the air
la	$1 / (5 + 8 \cdot \text{sqrt}(v))$	m ² K/W	Air heat insulation, including radiation
da	$\text{lambda} / (8 \cdot \text{sqrt}(v))$	m	Air vapour resistance
d	da+dcl	m	Total vapour resistance

³ In the SCOPE implementation this is replaced by the Dubois and Dubois (1916) formula: $A = 0.202 \cdot W^{0.425} \cdot S^{0.725}$ (m²) if W and S are known.

⁴ Although a constant for the thermal model this is in the SCOPE simulation software a variable that has to be specified in the scenario.

Table 8 Internal stimuli are calculated and used to produce shivering and skin by blood flow (SKBF), sweat rate, resulting skin vapour concentration and water production by metabolism. From the skin blood flow, the thermal conductance BC between core and skin is calculated.

Variable	Calculation	Unit	Description
offset	$0.2 - 0.4 \cdot \text{fit} - 0.25 \cdot \text{acclim}$	nd	Offset due to acclimatization and fitness
wc	$T_c - T_{\text{cref}} - \text{offset}$	°C	hot stimulus from the core ⁵
cc	$T_{\text{cref}} - T_c + \text{offset}$	°C	cold stimulus from the core ³
wsk	$T_{\text{sk}} - T_{\text{skref}}$	°C	hot stimulus from the skin ³
csk	$T_{\text{skref}} - T_{\text{sk}}$	°C	cold stimulus from the skin ³
shiv	$A \cdot 18 \cdot \text{csk} \cdot \text{cc}$	W	heat production by shivering ⁶
SKBF	$(6.3 + 45 \cdot \text{wc}) / (1 + 0.1 \cdot \text{csk}) \cdot 2^{\text{wsk}/6}$	l/m ² min	skin blood flow ⁷
BC	$A \cdot (6.5 + 0.7 \cdot \text{SKBF})$	W/K	heat conduction between core and shell
Gainsw	$(0.65 + 0.7 \cdot \text{fit}) \cdot (1 + 0.15 \cdot \text{acclim})$	nd	Effect of fitness and acclim. on sensitivity of the sweat function
SwR	$0.004 \cdot \text{Gainsw} \cdot (11 \cdot \text{wc} + (T_{\text{sk}} - T_{\text{skref}})) \cdot 10^{(\text{wc}/10.7)}$	g/m ² s	Sweat rate ⁸
Csk	$\text{Sat}(T_{\text{sk}}) \text{ or } d \cdot \text{SwR} / D + C_a$ (take smallest)	g/m ³	vapour concentration at skin, either physically limited (saturation) or limited by sweat production rate
Waterprod	$108 \cdot \Psi_{\text{work}} / (3.15 \cdot 10^6)$	g/s	water produced by metabolism (1 Mol of glucose produces 6 Mol of water and 3.15 MJ)

Table 9 The total heat capacity of the body is split in core and skin parts.

Variable	Calculation	Unit	Description
Cap	$3500 \cdot W$	J/K	total body heat capacity
alpha	$0.09 + 0.37 / (\text{SKBF} + 0.59)$	-	factor splitting core and shell
Capsk	$\text{alpha} \cdot \text{Cap}$	J/K	heat capacity of skin compartment
Capc	$(1 - \text{alpha}) \cdot \text{Cap}$	J/K	heat capacity of core compartment

4.1.2.3 Calculation of the heat balance (in W) and temperature changes

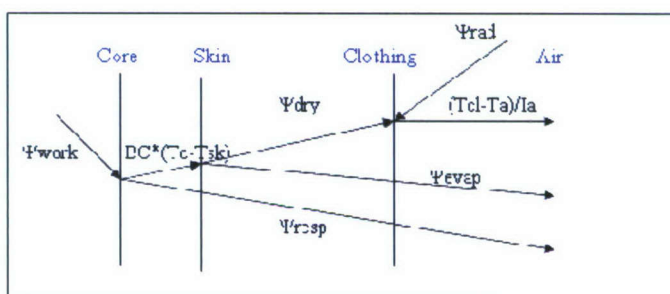


Figure 22 Heat flows in the thermal system.

Figure 22 shows how the heat flows interact between the nodes core, skin, clothing surface and air. Core and skin have heat storage capabilities. Heat storage capability of clothing is neglected because it is so much smaller than that of the body.

At the clothing surface, the clothing temperature is controlled by the dry heat flow from the skin, the incoming radiation and the heat flow from clothing to air. At the skin, heat is transported from the core and lost as dry heat to the clothing and evaporative heat.

⁵ If the value of this variable is lower than 0, then the value is set to 0.

⁶ Shivering is limited to a value of $A \cdot 225$.

⁷ Skin blood flow is limited to the values ranging from 0.5 to $90 \cdot (0.75 + 0.5 \cdot \text{acclim} + 0.66 \cdot \text{fit})$.

⁸ Sweat rate is limited to $0.222 \cdot (0.75 + 0.25 \cdot \text{acclim} + 0.5 \cdot \text{fit})$.

Condensation in the clothing is neglected and thus, the vapour escapes right into the air. At the core, heat is generated by work rate and shivering, and lost in a conductive way to the skin and both as dry and evaporative heat through the respiratory pathway. Mind that skin and core involve heat capacities and thus change incrementally, whereas the clothing temperature is calculated instantaneously, as a consequence of skin and air condition (see Table 10).

Table 10 Calculation of the heat balance (in W) and temperature changes.

Variable	Calculation	Description
Ψ_{work}	$WR + \text{shiv}$	Total heat production
Ψ_{rad}	$A \cdot 0.3 \cdot \epsilon \cdot \text{sun}$	Solar heat gain with 30% body exposed
Ψ_{evap}	$A \cdot H_e \cdot D \cdot (C_{\text{sk}} - C_a) / d$	Evaporation
Ψ_{dry}	$A \cdot (T_{\text{sk}} - T_{\text{cl}}) / I_{\text{cl}}$	Dry heat flow through clothing
Ψ_{respd}	$\Psi_{\text{work}} \cdot 0.0014 \cdot (34 - T_a)$	Respiratory dry heat loss
Ψ_{resp}	$\Psi_{\text{work}} \cdot 0.0027 \cdot (38 - C_a)$	Respiratory evaporation
dT_c	$dt \cdot (\Psi_{\text{work}} - BC \cdot (T_c - T_{\text{sk}}) - \Psi_{\text{respe}} - \Psi_{\text{respd}}) / \text{Capc}$	Core temp. rise during dt
dT_{sk}	$dt \cdot (BC \cdot (T_c - T_{\text{sk}}) - \Psi_{\text{dry}} - \Psi_{\text{evap}}) / \text{Capsk}$	Skin temp. rise during dt
T_{cl}	$T_a + I_a \cdot (Y_{\text{dry}} + Y_{\text{rad}}) / A$	Clothing temp. while radiated

4.1.2.4 New thermal condition

At each time step the parameters are updated. An additional feature is the drinking routine. Subjects get thirsty when dehydration is more than 1% of body weight. They start drinking at 1 l/hr if water is available.

Table 11 Calculation of the new thermal condition.

Variable	Update procedure	Unit	Description
T_c	$T_c + dT_c$	C	Dynamic core temp (see Table 10)
T_{sk}	$T_{\text{sk}} + dT_{\text{sk}}$	C	Dynamic skin temp (see Table 10)
BHC	$(\text{Capc} \cdot (T_c - T_{\text{cref}}) + \text{Capsk} \cdot (T_{\text{sk}} - T_{\text{skref}})) / (1000 \cdot W)$	J/g	Dynamic average body heat content
dehydration	$\text{dehydration} + dt \cdot (A \cdot S_{\text{wR}} + \Psi_{\text{respe}} / H_e - \text{Waterprod}) / 1000$	l	Cumulative dehydration

4.1.2.5 Performance effects

The way performance is degraded is described in Section 2.3.1.3. The outputs from the thermal model used to modify performance are body heat content, dehydration and shivering. The two first force subjects to stop activity, or to reduce the intensity of physical work, shivering may affect motor performance while still allowing other activities. In fact, increased work may resolve shivering.

The following thresholds are used for the definition of stress related to the thermal model:

- If $BHC < -20$ or if $BHC > 10$ J/g body mass then incapacitation follows (higher tolerance for cooling (as found by Lotens, 1978)).
- If dehydration $> 5\%$ of the body weight, then incapacitation follows.
- If $\text{shiv} > 0$ then no fine motor tasks due to shaking (Shivering prevents fine motor tasks).

4.1.2.6 Validation

The Gagge model is the follow up of the Stolwijk model, developed to support NASA with its design for space suits (Stolwijk, 1971). The Gagge model was a simplification, reducing the number of control variables and reducing the number of compartments

from 25 to 2. Gagge and Nishi used the two-node model for comfort studies and it was adopted by the ASHRAE as a standard (Gagge et al, 1971). Some of the physiological parameters in it are not completely realistic (such as the 90 l/min maximal skin blood flow for an adult male), but more importantly, it produces correct outcomes. Lotens and Havenith adopted this model for clothing studies. Lotens (1993) replaced the simple clothing algorithm by a more sophisticated layered clothing algorithm, allowing for a wide variety of ensembles, including reflective, transparent, hygroscopic, impermeable and other layers. Even the complex ensembles describe quite accurately the thermal responses registered in the climatic chambers on subjects. Havenith (1997) was more interested in individual variations between thermal responses and inserted some variables to deal with body size, acclimatization, gender and fitness effects. The two-node model worked fine also in these specialized conditions, be it that the blood flow and set point parameters had to be adjusted. This is a well established physiological fact (Havenith, 1997). In the current model, the clothing algorithm is simplified again, to somewhere between the Gagge and the Lotens version. Obviously, some details will be lost, rewarded by easier handling. However, the major conclusion is that this class of clothing algorithms, combined with the two-node physiological model has a great deal of validity if soaked clothing is avoided (by rain or sweat).

4.2 Metabolic System

The metabolic processes involved in physical work regard phosphor, glucose, lactate and fat. The phosphoric cycle is an immediate energy release employed for brief, explosive tasks. This is neglected here, as it relates to performances at a level of detail that is beyond the scope of SCOPE.

Glucose is the fuel for the other metabolic cycles, released from the intestines while metabolising food components like sugar or carbohydrates. At moderate work rates glucose is in an aerobic way metabolised in CO₂ and water. The water stays in the system, while CO₂ escapes by respiration. Glucose is like a fuel, stored in the muscles and liver and replenished by the intestines.

Fat is also metabolized, in particular when glycogen is less available, thus in prolonged exhaustive work (Guyton and Hall, 2000). The contribution of fat to the energy supply depends on the diet. Subjects with a fat diet burn relatively more fat.

At higher work rates, the aerobic metabolism is short in power and an anaerobic process supplies additional power. Glucose is converted to lactate at high rates and with limited efficiency. The split of work rate in aerobic and anaerobic parts depends also on fitness (see Figure 25). Fit persons produce less lactate and have a higher aerobic capacity.

Lactate is not only a waste product, but is itself also a fuel. However, it burns too slow to cater for high work rates and is consumed elsewhere in the body.

The build-up of lactate concentration in the muscle hurts and sets a tolerance limit.

Lactate is removed from the muscle by blood, to be metabolized in other organs, notably the liver and other, moderately hard working muscles.

Also lack of glucose is a work stopper, for two reasons. The first is that depletion of glucose slows the metabolic rate and the other is that it also lames the innervations of the muscle.

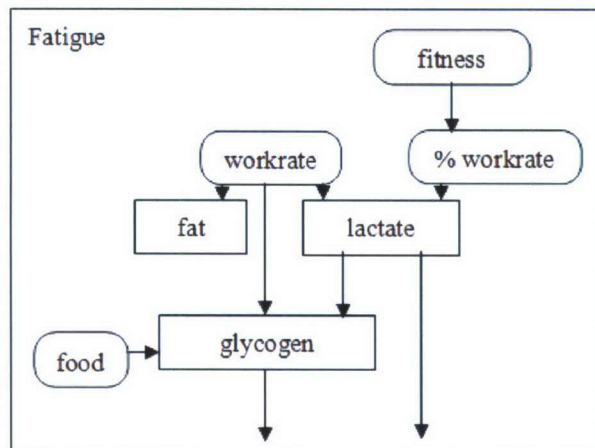


Figure 23 Scheme for glucose consumption and lactate production. The energy for the work rate is delivered by the metabolism of fat and glucose, producing lactate and CO₂.

We built the model thus on the monitoring of glucose and lactate, which makes it useful for tasks ranging in duration from 1 minute up to many hours. Factors influencing the glucose and lactate levels are the energy demand of the task, the fitness of the subject and the food regime (Figure 23).

4.2.1 A dynamic model of metabolism

The organs involved in the metabolism, as modelled here, are the intestines, delivering fuel, the muscles that consume fuel and produce lactate, the muscles that consume lactate and the liver that holds energy stores. The organs are connected through the blood flow. The distinction between the muscle groups is that in any type of activity some muscles are active and some other are not used. Actually, not used is not the right expression, they are used at a lower level of effort. We thus discern two muscle compartments.

Figure 24 shows the various body compartments involved in metabolism. The intestines provide a flow of glucose to the circulating blood. Blood is the carrier for glucose and lactate alike. Glucose is stored in the liver as glycogen, from which it can be retrieved and transported to the muscles. It is also stored in the muscles itself, but this is irreversible. Muscle glycogen can only be routed to the cells that metabolise it, but not back into the blood flow.

If the muscle works hard enough, lactate is formed in the muscle and washed out by the blood flow. From there, it may be used by the other, hard working muscles or converted to glycogen in the liver. This route is the backdoor to get lactate in the loop again as glucose.

Fat (fatty acids) is supposed to be abundantly available and a proportion of the energy is delivered by burning fat. This proportion depends on the availability of glycogen. Burning fat takes more oxygen than burning glucose and consequently when oxygen availability is the limitation, glycogen is used preferentially. At lower work rates, burning fat is substantial and certainly so when glycogen is nearly depleted. However, fat metabolism can not replace glycogen metabolism because it lacks speed.

The scheme of Figure 24 comprises five basic differential equations, for:

- blood glucose;
- blood lactate;
- working muscle glucose;
- working muscle lactate;
- other muscle glucose.

The biochemical processes involved are usually complicated, as they are assisted by catalysts and are active processes rather than diffusion processes. However, to simplify the description, we will assume that the reactions are biochemical reactions with typical speed constants. The other timing factor is the muscle blood flow, which depends on the work the muscle is performing and the need for restoration of glycogen stores.

The differential equations are specified in detail in Section 4.2.2.4.

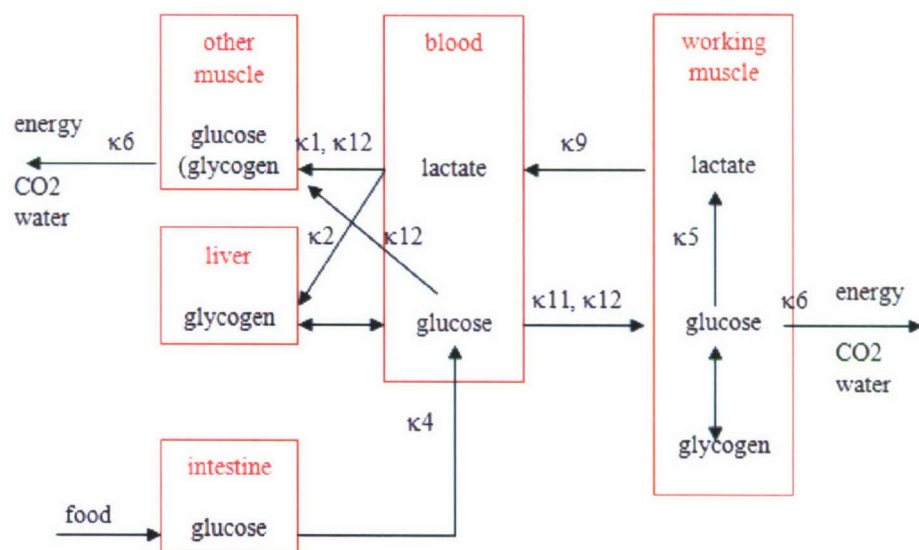


Figure 24 Formal scheme for metabolism, with reaction speed constants.

4.2.2 Algorithm

Below, the variables and equations are explained. See Table 12 for a definition of the subscripts used.

Table 12 The subscripts as used in the following sections.

Subscript	Description
O	Other muscle than involved in activity
W	Working muscle
aer	aerobic
max	maximal
min	minimal
ana	anaerobic
Gly	Glycogen
Glu	Glucose
La	Lactate
blood	blood
muscle	muscle
liver	liver

4.2.2.1 Constants and variables

We draw the constants from the literature and relate them to body weight. This is common practice in exercise physiology, as much of the inter subject variance is resolved by proportionality to body weight.

Table 13 The constants used in the metabolic model. W stands for body weight.

Constant	Value	Unit	Description
W_m	$W/3$	kg	Muscle weight (one third of weight)
$Cap_{\text{muscle, Gly}}$	$20 \cdot W_m$	l	Capacity to hold glycogen in muscle (Hargraves 2004) ⁹
$Cap_{\text{muscle, Glu}}$	W_m	l	Capacity to hold glucose in muscle
$Cap_{\text{muscle, La}}$	W_m	l	Capacity to hold lactate in muscle
$Cap_{\text{liver, Gly}}$	$1.3 \cdot W$	l	Capacity to hold glycogen in liver Nilsson (1973)
V_{bl}	$0.08 \cdot W$	l	Blood volume
$Cap_{\text{blood, Glu}}$	V_{bl}	l	Capacity to hold glucose in blood
$Cap_{\text{blood, La}}$	V_{bl}	l	Capacity to hold lactate in blood
$C_{\text{blood, Glu, max}}$	6.0	mMol/l	Blood glucose in rest (Guyton and Hall, 2000)
$C_{\text{blood, La, min}}$	1.0	mMol/l	Blood lactate in rest (Guyton and Hall, 2000)
$\delta'_{\text{Glu-La}}$	0.5	mMol/mMol	Glucose to lactate molecular ratio
R	18/19	no dimension	Lactate to glucose energy production ratio
κ_6	1/2880	mMol/J	Glucose metabolic energy equivalent (Guyton and Hall, 2000)
κ_4	0.09	mMol/s	Maximal glucose production rate ($prod_{\text{glu, max}}$) ¹⁰

Table 14 The constants defining the dynamics of the system, as found by adjusting model performance to experimental data (see Section 4.2.2.8).

Constant	Value	Unit	Description
κ_1	0.6	no dimension	Reaction velocity of lactate in other muscle
κ_2	0.015	l/s	Reaction velocity of lactate in liver ¹¹
κ_9	1/8	l/s	Muscle lactate transport rate
κ_{11}	0.4	no dimension	Muscle glucose transport rate
κ_{12}	2.0	l ² /(mMol/s)	Blood flow rate during recovery

Two conditions are introduced to ascertain that glucose can enter the muscle, but not return to the blood stream:

- $\kappa_8 = 1$ if $C_{\text{blood, Glu}} - C_{W\text{muscle, Glu}} > 0$, else 0 (nd).
- $\kappa_{10} = 1$ if $C_{\text{blood, Glu}} - C_{O\text{muscle, Glu}} > 0$, else 0 (nd).

Table 15 The variables in the metabolic model.

Category	Variable	Unit	Description
Input	WR	W	Work rate
	μ	no dimension	Fraction working muscle ($0.2 < \mu < 0.8$)
	fitness	no dimension	Relative fitness (0-1, max 1.5 for top athletes)
Intermediate	Bfl	l/s	Perfusion of muscles
	C	mMol/l	Concentration
	Cap	l	Capacity to store substance
Conditional	κ_8	no dimension	

⁹ In the SCOPE implementation, the effect of fitness is expressed by replacing the fixed factor of 20 by $(10 + 10 \cdot \text{fitness})$, see Section 4.2.2.5.

¹⁰ Given that food is available in the stomach. Food consumption is $prod_{\text{glu, max}} \cdot 0.36$.

¹¹ Note that the formulas involving κ_1 and κ_2 are different.

4.2.2.2 Work rate

The total work rate WR consists of anaerobic work WR_{ana} , aerobic work by working muscle $WR_{aer,W}$ and aerobic work by other muscle $WR_{aer,O}$. Other is not the same as inactive. It means that the other muscles perform moderate or light work and may burn lactate. How much work the other muscles perform depends on the user specified work distribution μ . 100 W is regarded as the basic metabolic rate. 20% of the work (above basic metabolic rate) is performed by the fraction $(1 - \mu)$ that is 'other', the other 80% is performed by the fraction μ working muscle. If μ is small, the working muscles work very hard and may produce lactate. To avoid extreme local muscle work, μ can't be smaller than 0.2. Otherwise the estimate of anaerobic work would be inadequate.

μ can not be larger than 0.8 as it is difficult to involve all muscles.

WR and μ are inputs from the task, $WR_{aer,max}$ and n are calculated from the fitness (see Section 4.2.2.5). Depending on the maximum aerobic capacity and the fitness, the fraction aerobic work is calculated as follows:

$$WR_{aer} = (WR^{-n} + WR_{aer,max}^{-n})^{-1/n}$$

This expression tells how well the aerobic capacity can be exploited. This goes better with trained subjects, thus with large n .

The work is now split in working and other muscles, assuming that other muscles are still performing 20% of the work, above the resting metabolism. Only working muscles are taxed to the level that anaerobic work is involved:

$$WR_{aer,O} = (1 - \mu) \cdot 100 + 0.2 \cdot (WR - 100)$$

$$WR_{aer,W} = WR_{aer} - WR_{aer,O}$$

$$WR_{ana} = WR - WR_{aer}$$

The fraction μ of the muscle mass is performing $WR_{aer,W}$ and WR_{ana} . According to the muscle mass, the capacities to contain glucose and lactate (see Section 4.2.2.4) are assigned. The blood flows through the muscle are 1.6 l/min per 100W of work rate. Resting muscle blood flow is 15% of 4 l/min = 0.6 l/min (Astrand and Rodahl, 2003). However, during recovery from exhaustive exercise, the blood flow is larger than the value in rest. Thus:

perfusion of working muscles (l/s):

$$Blf_W = (\mu \cdot (0.6 + \kappa_{12} \cdot (C_{blood,Glu,max} - C_{Wmuscle,Glu})) + 0.8 \cdot (WR - 100) / 100 \cdot 1.6) / 60$$

perfusion of other muscles (l/s):

$$Blf_O = ((1 - \mu) \cdot (0.6 + \kappa_{12} \cdot (C_{blood,Glu,max} - C_{Omuscle,Glu})) + 0.2 \cdot (WR - 100) / 100 \cdot 1.6) / 60$$

4.2.2.3 Reaction speeds

We define the capacities Cap for storage of glycogen (Gly), glucose (Glu) and lactate (La), in the blood, working muscles and liver as follows:

$$Flow = Cap \cdot dC/dt \text{ with dimensions } m\text{Mol/s} = (l) \cdot (m\text{Mol/l}) / (s)$$

Thus the dimension of capacity is litres: l of body tissue or l of blood or equivalent litres for high density storage like glycogen storage. Capacities are filled or depleted by flows, stemming from transport processes.

Most transports are the result of biochemical reactions, converting source substances into products with certain reaction speeds. We assume that for one way reactions the reaction is accelerated by supply of the source substance, but not decelerated by the product substance:

$$\text{Flow} = \kappa \cdot \Delta C_{\text{source}}$$

The substances here are glucose and lactate. Neither in the glucose to lactate conversion, or the other way around, is there a direct way back. In the working muscle, the rate of lactate production depends on the work rate, not on the glucose supply. In the other muscle and the liver, lactate is consumed in proportion to the lactate supply. Despite the fact that lactate is both directly metabolized in the other muscle and converted to other muscle glucose, we assume that glucose is formed first and then consumed. This is easier to handle.

$$\text{Flow} = \kappa \cdot \Delta C_{\text{source}} \cdot \delta C_{\text{prod}} / \delta C_{\text{source}} = \kappa \cdot \Delta C_{\text{source}} \cdot \delta'$$

The partial differential $\delta C_{\text{prod}} / \delta C_{\text{source}}$ is called δ' and can be drawn from the reaction equation. For the lactate to glucose conversion, 2 mMol of lactate equals 1 mMol of glucose and $\delta'_{\text{Glu-La}} = 1/2$.

The reaction speed for glucose-glycogen conversion is so high that we will assume that glycogen and glucose are always in equilibrium. Although we explicitly model muscle glucose, in reality the glucose freed from the glycogen is metabolized immediately. Glycogen acts as condensed glucose, increasing effectively the capacity for glucose rather than involving another reaction with associated dynamics. In Figure 24 the associated reaction speeds are left out for this reason.

The reactions are:

- *Lactate uptake by other muscle:* $\kappa 1 \cdot R \cdot (C_{\text{blood,La}} - C_{\text{blood,La,min}}) \cdot \delta'_{\text{Glu-La}} \cdot \text{Blfl}_O$.
Because no lactate metabolism is simulated, lactate is virtually converted to glucose and added to the other muscle glucose pool. The transport depends both on the bloodflow and the lactate concentration, because these constitute together the supply. Only the fraction $(1-\mu)$ of the muscle is 'other', hence the transport also depends on μ .
- *Blood lactate uptake through liver:* $\kappa 2 \cdot (C_{\text{blood,La}} - C_{\text{blood,La,min}})$.
Lactate is converted to liver glucose and glycogen, in proportion to the supply rate. The liver takes up lactate regardless of the need for glucose.
- *Constant inflow of glucose from intestine:* $\kappa 4$.
This is the maximum. On an empty stomach this figure will decrease. We assume that it falls back to zero, although this is not fully realistic because the body eats up itself during prolonged starvation. The fat and protein involved is handled through the muscle equation. Excess glucose production is converted to body fat. In theory body fat is another fuel pool to monitor, but this pool is so large, that it is infinite for practical purposes. We thus do not keep track of body fat.
- *Aerobic uptake of glucose:* $\kappa 6 \cdot \text{WR}_{\text{aer}} \cdot (0.5 + 0.5 \cdot C_{\text{muscle,Glu}} / C_{\text{blood,Glu,max}})$.
This is a direct relationship because the power that is requested needs to be catered for in terms of fuel, or it will drop. Glucose is not the only fuel. As glycogen is depleted, progressively fatty acids and amino acids are metabolized. However, they are not a complete substitution. The expression here is an approximation of the part of the power that is fueled by glycogen (Guyton and Hall, 2000, p 972).
- *Anaerobic uptake of glucose:* $\kappa 6 \cdot \text{WR}_{\text{ana}} / (1-R)$.
This is a direct relationship. The efficiency is the factor $1/(1-R)$ less than of the aerobic process. Fat metabolism does not produce significant lactate.
- *Glucose flow to muscle:* $\kappa 11 \cdot \text{Blfl} \cdot (C_{\text{blood,Glu}} - C_{\text{muscle,Glu}})$ (if $C_{\text{blood,Glu}} > C_{\text{muscle,Glu}}$, else 0).
The transport is dependent on muscle perfusion.
- *Lactate flow from muscle to blood:* $\kappa 9 \cdot (C_{\text{muscle,La}} - C_{\text{blood,La}})$.
The transport over the cell membrane is slower than the blood can take up and becomes the critical factor.

In the above equations R accounts for the fact that a small part of the intrinsic energy of glucose is freed in the splitting into lactate. The consequence is that there is a large turnover of glucose and lactate in the anaerobic energy production.

4.2.2.4 Differential equations

We now use the following basic differential equation (mass conservation law in Mmol/s) for a compartment with the concentration C and capacity Cap:

$$\text{Cap} \cdot dC/dt = (\text{sources} + \text{inflow}) - (\text{drains} + \text{outflow})$$

for the various compartments in Figure 24, specified in detail as follows:

Blood glucose

The sources are glucose from food and lactate from blood, converted in the liver to glucose, and the drains are the glucose uptakes from working and other muscles.

$$(\text{Cap}_{\text{blood,Glu}} + \text{Cap}_{\text{liver,Gly}}) \cdot dC_{\text{blood,Glu}}/dt = \kappa 4 - \kappa 8 \cdot \kappa 11 \cdot \text{Bfl}_W \cdot (C_{\text{blood,Glu}} - C_{W\text{muscle,Glu}}) - \text{Bfl}_O \cdot \kappa 10 \cdot \kappa 11 \cdot (C_{\text{blood,Glu}} - C_{O\text{muscle,Glu}}) + \kappa 2 \cdot R \cdot (C_{\text{blood,La}} - C_{\text{min}}) \cdot \delta'_{\text{Glu-La}} \quad (1)$$

Glucose is produced, provided enough food is available. More food will not increase the glucose production. Also, blood glucose concentration is bound to a maximum and additional glucose production will be stored as fat, which is too slow to play a role here. For every 32 mg of food, 16 mg of glucose is produced, which is $16/180 = 0.09$ mMol of glucose. This is the food consumption and glucose production for every second. Thus food is consumed at 32 mg/s when glucose is produced at 0.09 mMol/s.

$$\kappa 4 = \text{prod}_{\text{glu,max}} \text{ when food} > 0 \text{ and } C_{\text{blood,Glu}} < C_{\text{blood,Glu,max}} \quad (2)$$

Thus the food mass in the stomach decreases every second with $2 \cdot \kappa 4 \cdot 0.18$ (g).

Equation 2 also assures that the resting value for $C_{\text{blood,Glu}}$ returns to $C_{\text{blood,Glu,max}}$.

Once glucose is in the muscle, there is no return. Therefore $\kappa 8$ is unity when $C_{\text{blood,Glu}}$ is larger than $C_{W\text{muscle,Glu}}$ and zero when smaller. R is the efficiency of recovery of glucose from lactate. Muscles mass is split in working and other muscles by the variable μ and each type of muscle has a work rate dependent blood perfusion. The other muscles (including heart and respiration) are not inactive, but rather work at a work rate in proportion to the total. WR_{ana} , WR_{aerW} and WR_{aerO} cast together the total work rate WR. The split of WR depends on relative workload and fitness, following the mechanism explained in Section 4.2.2.3. The work rate and blood flow are split in working and other muscle compartments, each consisting of a basic rate and a work bound rate on top. This assures that when the work rate drops, working muscle is smoothly changed into resting muscle. The significance of μ is that the working muscle work rate is fully assigned to the part μ of the muscle mass. The associated changes are that the capacity depends on μ , but also the exchange surface for lactate. Those transports that depend on work rate or blood flow have the effect of μ already taken into account in the work rate and blood flow. Obviously, the smaller μ is, the higher the load is on the few working muscles. This is limited by involving at least 20% of muscle mass in an activity. The model does not recognize that local loads may cause lactate production at levels of work rate that over all would not do so.

Working muscle glucose

The source is glucose from blood and the drains are aerobic and anaerobic glucose metabolism.

$$\begin{aligned} \mu \cdot (\text{Cap}_{\text{muscle, Glu}} + \text{Cap}_{\text{muscle, Gly}}) \cdot dC_{\text{Wmuscle, Glu}}/dt = & \kappa 8 \cdot \kappa 11 \cdot \text{Blfl}_W \cdot \\ & (C_{\text{blood, Glu}} - C_{\text{Wmuscle, Glu}}) - \kappa 6 \cdot \text{WR}_{\text{ana}} / (1-R) - \kappa 6 \cdot \text{WR}_{\text{aerW}} \cdot \\ & (0.5+0.5 \cdot C_{\text{Wmuscle, Glu}} / C_{\text{blood, Glu, max}}) \end{aligned} \quad (3)$$

Other muscle glucose

The sources are glucose from blood and lactate from blood and the drain is aerobic glucose metabolism.

$$\begin{aligned} (1-\mu) \cdot (\text{Cap}_{\text{muscle, Glu}} + \text{Cap}_{\text{muscle, Gly}}) \cdot dC_{\text{Omuscle, Glu}}/dt = & \text{Blfl}_O \cdot \kappa 10 \cdot \kappa 11 \cdot (C_{\text{blood, Glu}} - \\ & C_{\text{Omuscle, Glu}}) + \kappa 1 \cdot R \cdot (C_{\text{blood, La}} - C_{\text{blood, La, min}}) \cdot \delta'_{\text{Glu-La}} \cdot \text{Blfl}_O - \kappa 6 \cdot \text{WR}_{\text{aerO}} \cdot (0.5+0.5 \cdot \\ & C_{\text{Omuscle, Glu}} / C_{\text{blood, Glu, max}}) \end{aligned} \quad (4)$$

Working muscle lactate

The source is lactate produced by anaerobic metabolism and the drain lactate to blood. We will assume that the lactate transport from the muscle cells to the blood has a time constant, depending on the amount of muscle involved, hence the factor μ in the drain. This time constant is relatively short since lactate transport over the cell membrane is facilitated and faster than simple diffusion:

$$\mu \cdot \text{Cap}_{\text{muscle, La}} \cdot dC_{\text{muscle, La}}/dt = \kappa 6 \cdot \text{WR}_{\text{ana}} / (1-R) / \delta'_{\text{Glu-La}} - \mu \cdot \kappa 9 \cdot (C_{\text{muscle, La}} - C_{\text{blood, La}}) \quad (5)$$

Blood lactate

The source is lactate produced by the anaerobic metabolism of the working muscle and the drains are lactate uptake by the other muscles and the liver.

$$\begin{aligned} \text{Cap}_{\text{blood, La}} \cdot dC_{\text{blood, La}}/dt = & \mu \cdot \kappa 9 \cdot (C_{\text{muscle, La}} - C_{\text{blood, La}}) - \kappa 1 \cdot (C_{\text{blood, La}} - C_{\text{blood, La, min}}) \cdot \delta'_{\text{Glu-La}} \cdot \\ & \text{Blfl}_O - \kappa 2 \cdot (C_{\text{blood, La}} - C_{\text{blood, La, min}}) \end{aligned} \quad (6)$$

where $C_{\text{blood, La, min}}$ is the resting value for $C_{\text{blood, La}}$. $\kappa 1$ converts lactate to (imaginary) muscle glucose, whereas $\kappa 2$ converts lactate through the liver into blood glucose. R accounts for the lactate that is used to provide the energy to convert the rest to glucose.

4.2.2.5 Effects of training

The effect of training is expressed in fitness, running from 0 (unfit) to 1 (very fit).

Specialized athletes may go as far as 1.5. Training works on various levels:

- Training improves the maximal aerobic work rate: $\text{WR}_{\text{aer, max}} = 14 \cdot W \cdot (0.5 + \text{fitness})$ (W) (this equates to 55 mMol of $\text{O}_2/\text{kg min}$, specified for well trained students by Astrand and Rodahl, 2003. Top athletes may have oxygen uptakes up to 80 mMol of $\text{O}_2/\text{kg min}$).
- Training decreases the percentage of anaerobic work: when working at $\text{WR} = \text{WR}_{\text{aer, max}}$, $p_{\text{ana}} = 16 - 10 \cdot \text{fitness}$. Athletes do not much better than the very fit and p_{ana} must be limited to at least 3.
- Training will increase the tolerable lactate concentration in the muscles: $C_{\text{muscle, La, max}} = 11 + 15 \cdot \text{fitness}$ (mMol/l).
- Training will increase the muscle glycogen storage: $\text{Cap}_{\text{muscle, Gly}} = (10 + 10 \cdot \text{fitness}) \cdot W_m \cdot (l)$.

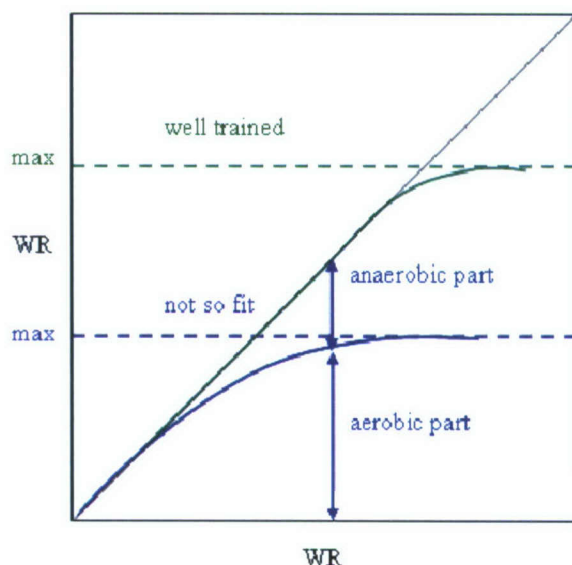


Figure 25 The work rate on the abscissa is split in aerobic and anaerobic parts on the ordinate. For a not so fit person a substantial part is anaerobic, which is not sustainable. For a well trained person the same work rate is completely aerobic and sustainable. Note that the vast difference in performance between trained and untrained is the combined effect of VO_{2max} and p_{ana} , sustaining about 50% of 500 W (250 W) for the untrained and 85% of 1500 W (almost 1300 W) for the well trained. Moreover, well trained persons employ the power more efficiently.

The total work rate (blue vertical in Figure 25) is split in an anaerobic and an aerobic part. Anaerobic metabolism starts to increase before the maximum aerobic work rate (dashed) is reached. For unfit persons this starts at 50% of the maximal aerobic work rate, while for fit persons it only starts at 85 or 90%. Fit persons also have a higher maximal aerobic work rate. Both effects combined lead to dramatically different lactate productions. In Figure 25 the fit person (green line) works completely aerobic, whereas the unfit person works for 30% anaerobic, a condition that he can sustain for probably only a few minutes. The curves of the aerobic part have the characteristic of:

$$WR_{aer} = (WR^{-n} + WR_{aer,max}^{-n})^{-1/n}$$

where n determines the sharpness of the bend. The best parameter for sharpness is the contribution of WR_{ana} to metabolism in % (p_{ana}) if $WR = WR_{aer,max}$:

$$n = 65 / p_{ana} = 65 / (16 - 10 \cdot \text{fitness}) \quad (n < 20)$$

For untrained persons n is about 4 and for trained persons about 11.

4.2.2.6 Calculations

Boundaries

if $C_{\text{blood,Glu}} > C_{\text{blood,Glu,max}}$ then $\kappa_4 = 0$

if $C_{\text{blood,Glu}} - C_{\text{Wmuscle,Glu}} > 0$, then $\kappa_8 = 1$, else $\kappa_8 = 0$

if $C_{\text{blood,Glu}} - C_{\text{Omuscle,Glu}} > 0$, then $\kappa_{10} = 1$, else $\kappa_{10} = 0$

if $(C_{\text{blood,La}} - C_{\text{blood,La,min}}) < 0$, then $\kappa_1 = 0$ and $\kappa_2 = 0$

Equations

$$C_{W\text{muscle,Glu}} = C_{W\text{muscle,Glu}} + (dt/(\mu \cdot (Cap_{\text{muscle,Glu}} + Cap_{\text{muscle,Gly}}))) \cdot (\kappa_8 \cdot Bl_{\text{flW}} \cdot \kappa_{11} \cdot (C_{\text{blood,Glu}} - C_{W\text{muscle,Glu}}) - \kappa_6 \cdot WR_{\text{ana}} / (1-R) - \kappa_6 \cdot WR_{\text{aerW}} \cdot (0.5 + 0.5 \cdot C_{W\text{muscle,Glu}} / C_{\text{blood,Glu,max}}))$$

$$C_{O\text{muscle,Glu}} = C_{O\text{muscle,Glu}} + (dt/((1-\mu) \cdot (Cap_{\text{muscle,Glu}} + Cap_{\text{muscle,Gly}}))) \cdot (Bl_{\text{flO}} \cdot \kappa_{10} \cdot \kappa_{11} \cdot (C_{\text{blood,Glu}} - C_{O\text{muscle,Glu}}) + \kappa_1 \cdot R \cdot Bl_{\text{flO}} \cdot \delta'_{\text{Glu-La}} \cdot (C_{\text{blood,La}} - C_{\text{blood,La,min}}) - \kappa_6 \cdot WR_{\text{aerO}} \cdot (0.5 + 0.5 \cdot C_{W\text{muscle,Glu}} / C_{\text{blood,Glu,max}}))$$

$$C_{\text{blood,Glu}} = C_{\text{blood,Glu}} + (dt/(Cap_{\text{blood,Glu}} + Cap_{\text{liver,Gly}})) \cdot (\kappa_4 - Bl_{\text{flW}} \cdot \kappa_8 \cdot \kappa_{11} \cdot (C_{\text{blood,Glu}} - C_{W\text{muscle,Glu}}) - Bl_{\text{flO}} \cdot \kappa_{10} \cdot \kappa_{11} \cdot (C_{\text{blood,Glu}} - C_{O\text{muscle,Glu}}) + \kappa_2 \cdot R \cdot (C_{\text{blood,La}} - C_{\text{min}}) \cdot \delta'_{\text{Glu-La}})$$

$$C_{\text{muscle,La}} = C_{\text{muscle,La}} + (dt/(\mu \cdot Cap_{\text{muscle,La}})) \cdot (\kappa_6 \cdot WR_{\text{ana}} / (\delta'_{\text{Glu-La}} \cdot (1-R)) - \mu \cdot \kappa_9 \cdot (C_{\text{muscle,La}} - C_{\text{blood,La}}))$$

$$C_{\text{blood,La}} = C_{\text{blood,La}} + (dt/Cap_{\text{blood,La}}) \cdot (\mu \cdot \kappa_9 \cdot (C_{\text{muscle,La}} - C_{\text{blood,La}}) - (\kappa_1 \cdot Bl_{\text{flO}} / \delta'_{\text{Glu-La}} + \kappa_2) \cdot (C_{\text{blood,La}} - C_{\text{blood,La,min}}))$$

4.2.2.7 Performance effects

The concentration of lactate and glucose in the muscles, and the concentration of glucose in the blood can affect performance.

Lactate concentration

Lactate build-up in the muscle will cause pain, resulting in a degradation of performance. When the lactate concentration is maximal then muscle performance will completely stop. The level of this maximum depends on the fitness of the person and is given by:

$$C_{\text{muscle,La,max}} = 11 + 15 \cdot \text{fitness (mMol/l)}$$

Blood glucose

If blood glucose drops, coordination fails due to nerve blocking. The gross motor, fine motor and cognitive functions are affected. The stress from glucose depletion is considered maximal when the level drops below 3.6: $C_{\text{blood,Glu,min}} = 3.6$ (mMol/l).

Muscle glucose

Work rate cannot be maintained if muscle glucose drops to 0: $C_{\text{muscle,Glu,min}} = 0$ (mMol/l). However, at a slower pace work can be continued on fat as a fuel.

4.2.2.8 Validation

The model is built on well researched physiological relationships, fed by well established clinical data. The validity depends on the sophistication of the relationships, the neglect of interactions and the estimates of parameters that are specific for the model. In particular, the model depends on estimates for κ_1 , κ_2 , κ_9 , κ_{11} and κ_{12} , controlling muscle lactate resorption, liver lactate resorption, working muscle lactate diffusion, muscle glucose absorption and recovery blood flow, respectively. The parameter values are found by matching the model outcomes with experimental data. This is a relatively small number of parameters for a model of this complexity.

The parameter μ , which is completely neglected in the physiological literature, is of great practical importance, since work performed by small muscle groups is far more exhaustive than the same amount of work involving large muscle groups. We assign 80% of the work rate to the working muscle mass (fraction μ) and 20% to the other muscle mass (fraction $1-\mu$). The lactate formed in the working muscles creates a higher concentration

in the muscle cells when less mass is involved and thus the tolerance is earlier reached. On the other hand, more other muscle mass is available to resorb the lactate, resulting in quicker removal. No useful experimental data was found for confirmation.

Another parameter, which is often not specified in the literature when reporting experimental data, is the fitness of the subjects. We solved this here by specifying fitness as a scale of 0 to 1, with values up to 1.5 for highly specialized athletes, while making the tolerance criteria subject to this fitness. This is a practical and intuitive way to deal with training states. The absolute work rate is used as model input. The user needs to interpret this in terms of performance. It is well known that trained subjects are not only fitter, but also more efficient. Trained subjects, for instance runners, can work at 55 ml of O₂ per kg body mass per minute, equivalent to a work rate of 1500 W. Extended work could be performed at 85% of this, 1300 W. The energy cost of experienced runners is about 280 J/m, independent of speed (Astrand and Rodahl, 2003, p 484), resulting together in a speed of almost 17 km/hr, which indeed is a fine performance, 35 min at the 10 km run.

The split of work rate in aerobic and anaerobic shares, summarized by Astrand and Rodahl on p 257 for athletes (max aerobic power of 1660 W) performing maximal work during varying times shows a general good similarity with the model data: 56% anaerobic during 1 min (A&R 68%), 46% during 2 min (50%), 10% during 10 min (13%), 3.7% during 30 min (4%) and 1.4% during 60 min (1.4%). The model shows some underestimation for short work bouts. However, A&R's data are not measured, but calculated and the model shows very high post exercise muscle lactate concentrations, whereas in the next paragraph the model lactate seems to fit well. There must be some inconsistency here in the data used as a reference.

Simulation of the example of a 295 kJ work bout over 2.6 min (Astrand and Rodahl, p 250) reveals muscle and blood glucose peaks of 25 and 17 mMol/l, respectively, the same as found experimentally. The decay time of blood lactate till 2 mMol/l is 70 min, as compared to 65 min experimentally. The fitness was not specified by Astrand and Rodahl, but we set it at .95, well trained. Although it is known that lactate diffusion from muscle to blood is facilitated by transporter cells, we neglected that effect, with the result that the approach to the resting condition is too slow in its final stages.

The effect of fitness on removal rate of lactate is under debate. This model indicates that there is an effect of training state on lactate washout, be it modest. The most significant difference is that fairly well trained subjects (fitness 0.8) have optimal removal rates at higher work rates (50% VO₂max) than less trained subjects (fitness 0.5, 30% VO₂max). This compares to the values collected by Astrand and Rodahl, 2003, p 255. The associated washout times are 23 minutes (while exercising), to 50 min (while resting), matching experimental values.

Depletion of muscle glycogen at 75% VO₂max exercise shows a linear decline (A&R, p 376), exhaustion following at exercise times proportional to the initial glycogen content (1 minute for every mMol/kg muscle, A&R p 379). When modelling 75% VO₂max work during 120 min, indeed the glycogen is depleted while blood glucose is approaching a critical value (64% of 6 mMol/l or 3.8 mMol/l, A&R p 376). The data of McArdle et al (2001) do not completely match with those of A&R, and the model shows good agreement at exercise till exhaustion at 63% and 150% of VO₂max, with slight deviations at 83% and 130%. It must be commented, however, that exhaustion times are highly dependent on fitness, which is not specified by McArdle et al (2001).

Restoration time after glycogen depletion is shorter for the liver than for the muscle tissue (McArdle et al, 2001). In trained subjects muscle glycogen is restored after 20 hr (McArdle, p 85 and 96), but seems inconsistent with the data on p 84, showing that the glycogen depletion of exhaustive work on successive days is not restored the next day. Guyton and Hall state that restoration takes 2 days for a carbohydrate rich diet and longer for a mixed diet. The glycogen restoration after depletion may continue over three days and show super compensation (160 mMol/kg after an initial 80 mMol/kg, A&R p 378). We have not modelled any effects of training over time and count on a 120 mMol/kg glycogen charge, which can effectively be used for 80 mMol/kg only. In our model liver glycogen is following the blood glucose level and indeed is restored much faster than the muscle glycogen. Resting muscle blood flow is an important factor in restoration of muscle glycogen and the reported resting muscle perfusion leads to slow restoration. We increased the resting blood flow in proportion to the need for restoration, which is in agreement with prolonged raised heart rates after strenuous exercise. Restoration time is now between 16 and 20 hours, depending on the depth of depletion. That may seem a little fast, but slowing it has more serious consequences for other performance aspects, and given the confusion in the literature this is the best solution for now.

4.3 Sleep deprivation

Main determinants of sleepiness are the diurnal phase (time of day relative to biologically adjusted cycle) and the sleep deficit. According to Belyavin and Spencer (2004) the effects are additive. Sleep deficit is expressed as the cumulative shortage compared to 6 hrs per 24. Time on task makes vigilance decrease and there is an interaction with sleep deficit, dropping performance faster with time on task for large deficits. Sleep deprivation works on vigilance through slowing of thinking and perceptual errors, resulting in overlooking of options and lower processing capacity. Automatic tasks are showing errors.

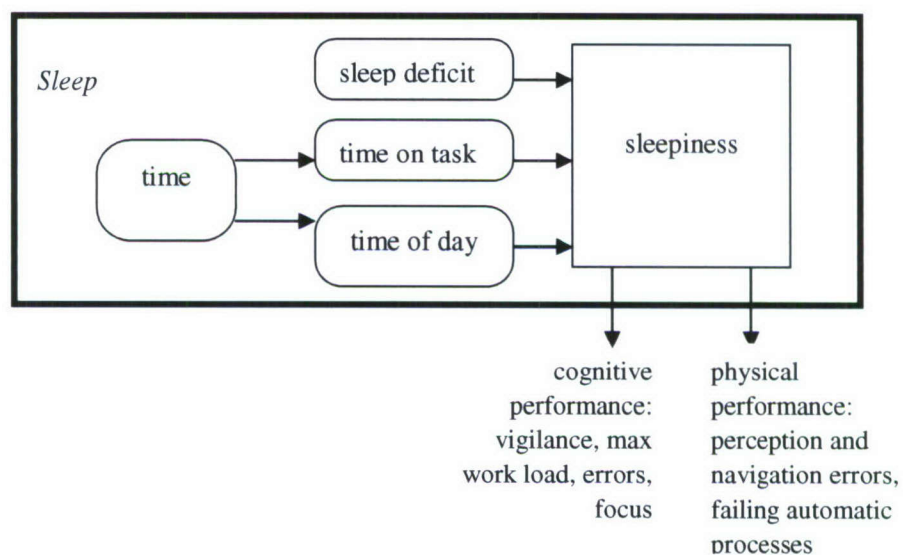


Figure 26 A simple sleep model.

4.3.1 Algorithm

The algorithm consists of four steps, namely determining the sleep deficit and the time of day, and use these as inputs to calculate γ , which is in turn used to calculate the sleepiness.

$$sleepdef = sleepdef_{init} + time / 4 - t_{sleep}$$

$$timeOfDay = (1 + \cos 2\pi((t - 14400) / 86400)) / 2$$

$$\gamma = \alpha \cdot timeOfDay + \beta \cdot sleepdef$$

$$sleepiness = 1 - e^{-\gamma}$$

with:

- *sleepdef*: sleep deficit relative to 6 hours of sleep per 24 hours.
- *timeOfDay*: time relative to diurnal cycle.
- *sleepiness*: mental state, deteriorating certain psychophysical functions.
- *sleep*: cumulative sleep time.

4.4 Future Work

4.4.1 Metabolic System

4.4.1.1 Fat burning

In the metabolic model the burning of fat is modelled indirectly by lowering the glucose consumption. However, when glycogen and glucose are completely depleted, fat can be used as the only source of energy. The current metabolic model does not account for this correctly since the burning of fat is not modelled *explicitly*. Explicitly modelling the burning of fat would require substantial modifications to the model.

The result of this simplification is that, although in the current implementation of SCOPE depletion of glucose will lead to lower physical task performance, the burning of glucose may still continue since moderate work remains possible. This could therefore result in negative glucose concentrations.

A solution for this problem could be the following: the effect of stress resulting from glucose depletion would have to be altered. Even without glucose a low work rate should have to be maintainable. The metabolic model would then also have to be adjusted in that if no glucose is available, all energy is produced from fat production. This can be achieved by altering the ratio between burning fat and carbohydrates, as given by the formula: $0.5 + 0.5 \cdot CW_{\text{muscle,Glu}} / C_{\text{blood,Glu,max}}$ (see updating mechanisms of working and other muscle glucose).

4.4.1.2 Load carrying

One physiological factor that is missing from SCOPE, but that is relevant from an operational performance perspective, is discomfort as a result of carrying heavy loads. Muscle aching, local tissue compression or local pain may cause the wearer to stop. Subjectively reported Rate of Perceived Exertion is a measure for immediate perception of load.

Ammonia concentration (a waste product of protein metabolism) in the tissue may be a measure for tolerance and so may lactate be. Lactate is formed if blood flow is blocked and aerobic metabolism fails. Due to the limited storage capacity of the muscle for lactate, pain may emerge quickly.

For now, we will not detail this in a model other than the distinction made between working and other muscle compartments. Maybe a relationship between tolerance time and weight carried during walking will be included in a future version of SCOPE.

4.4.2 *Sleep Deprivation*

In a previous version of SCOPE sleep deprivation was linked to the time an entity was performing a task (γ was multiplied by the time on task). This is however not a very useful factor since different tasks have very different effects on sleepiness. It might be better to directly couple the cognitive and physical workload as specified in the pandemonium with the model of sleep deprivation. Also, the effects of sleep deprivation are at the moment not modelled sufficiently. It should however be easy to model these effects by affecting some of the pandemonium resources and thereby indirectly affecting task performance.

5 Weapon effects

The weapon effects model of SCOPE is about to be overhauled, so much of the following is likely to change in the future. This document will be maintained to keep reflecting the current state of the models in SCOPE.

Presently the weapon effects model in SCOPE is a continuous model in which a group has a slowly decreasing size when under attack. In this model the group is always attacked 'as a group', i.e. even though the chances of a hit are calculated on a person-to-person basis, the effects are averaged over the group. The new model will keep an administration of damage per individual in the group.

5.1 Weaponry models

Two types of weapons effects (powers) are modelled in SCOPE: direct and indirect. Direct powers must be aimed (directed) at their target (e.g. a rifle) while an indirect power delivers a threat in a circular area surrounding the detonation point (e.g. a hand grenade). Indirect powers can be fragmenting, doing damage by spreading fragments over the impact range; non-fragmenting indirect powers deliver a continuous pressure over the impact range.

Finally SCOPE has hand launched weapons, this category is used to indicate that the whole weapon is spent during use, instead of spending ammunition and keeping the weapon, again the hand grenade is an example of this category.

Continuous powers can be both indirect and direct, with a high explosive grenade as an example of an indirect continuous power, and a flamethrower as an example of a continuous directed power. Continuous powers differ from fragmenting powers in the sense that fragmenting powers only result in a chance of being impacted (the fragments could miss), while continuous powers deliver a continuous threat and any exposed area is impacted with certainty.

5.1.1 Weapons

Weapons are defined by a range of parameters:

Table 16 Weapon parameters.

Parameter	Denotes [units]
Name	The name of this type of weapon, used in scenarios
Weaponry type	FIREARM or HANDLAUNCHED
Is direct	TRUE for direct weapons
Ammunition	The amount of ammunition that can be held in the weapon
Tau	Action range of the weapon [m], e.g. 0.01 for gun, 10 for grenade
Nf	Number of fragments, passing a hemisphere of $2\pi d^2$ area
Aiming	Aiming accuracy in arc minutes [arcmin]
Minreach	Minimal distance at which the weapon is effective [m]
Maxreach1	Idem for areas protected with Type I protection
Maxreach2	Idem for areas protected with Type II protection
Maxreach3	Idem for areas protected with Type III protection
Maxreach4	Idem for areas protected with Type IV protection
Apply rate	Frequency of 'shots' per second [1/s]
Response time	Time between order to apply and taking effect [s]
Is continuous	TRUE or FALSE, indicating if the power is continuous
Weight	Weight of weapon [kg]

5.2 Ballistic protection

Ballistic protection is classified according to the United States National Institute of Justice, as described in the NIJ Standard 0101.04. This standard has four (main) classes of protection, Type I through IV in SCOPE. The classes are described below¹²:

Table 17 Ballistic protection classification.

Type 1	This armour protects against .22 calibre Long Rifle Lead Round Nose (LR LRN) bullets, with nominal masses of 2.6 g (40 gr) impacting at a maximum velocity of 320 m/s (1050 ft/s) or less, and .380 ACP Full Metal Jacketed Round Nose (FMJ RN) bullets, with nominal masses of 6.2 g (95 gr) impacting at a maximum velocity of 312 m/s (1025 ft/s) or less.
Type 2a	This armour protects against 9 mm Full Metal Jacketed Round Nose (FMJ RN) bullets, with nominal masses of 8.0 g (124 gr) impacting at a maximum velocity of 332 m/s (1090 ft/s) or less, and .40 S&W calibre Full Metal Jacketed (FMJ) bullets, with nominal masses of 11.7 g (180 gr) impacting at a maximum velocity of 312 m/s (1025 ft/s) or less. It also provides protection against the threats mentioned in [Type 1].
Type 2	This armour protects against 9 mm Full Metal Jacketed Round Nose (FMJ RN) bullets, with nominal masses of 8.0 g (124 gr) impacting at a maximum velocity of 358 m/s (1175 ft/s) or less, and 357 Magnum Jacketed Soft Point (JSP) bullets, with nominal masses of 10.2 g (158 gr) impacting at a maximum velocity of 427 m/s (1400 ft/s) or less. It also provides protection against the threats mentioned in [Types 1 and 2a].
Type 3a	This armour protects against 9 mm Full Metal Jacketed Round Nose (FMJ RN) bullets, with nominal masses of 8.0 g (124 gr) impacting at a maximum velocity of 427 m/s (1400 ft/s) or less, and .44 Magnum Semi Jacketed Hollow Point (SJHP) bullets, with nominal masses of 15.6 g (240 gr) impacting at a maximum velocity of 427 m/s (1400 ft/s) or less. It also provides protection against most handgun threats, as well as the threats mentioned in [Types 1, 2a, and 2].
Type 3	This armour protects against 7.62 mm Full Metal Jacketed (FMJ) bullets (U.S. Military designation M80), with nominal masses of 9.6 g (148 gr) impacting at a maximum velocity of 838 m/s (2750 ft/s) or less (provided the projectile hits the hard trauma plate insert). It also provides protection against the threats mentioned in [Types 1, 2a, 2, and 3a].
Type 4	This armour protects against .30 calibre armour piercing (AP) bullets (U.S. Military designation M2 AP), with nominal masses of 10.8 g (166 gr) impacting at a maximum velocity of 869 m/s (2850 ft/s) or less (provided the projectile hits the hard trauma plate). It also provides at least single hit protection against the threats mentioned in [Types 1, 2a, 2, 3a, and 3].

In SCOPE the types 2a and 2 together form type II (2) and 3a and 3 together form type III (3).

This ballistic protection classification assumes that bullets hit at their maximum speed. This is of course not always the case, the distance from which the shot is fired determines the speed at impact. This means that the distance is also a parameter for the amount of protection.

To encode all these parameters, the level of protection is stored for each power (weapon). The type of protection worn by a target determines the maximum range of a power. An unprotected target means that the standard maximum is used. But when the target is protected, this lowers the maximum range of the power, since longer distance means lower velocity and a certain velocity is needed to penetrate the protection. For each power, five maximum reach values are stored, one for unprotected areas, and then one for each type of protection (1 through 4).

When a person (entity) in SCOPE is wearing ballistic protection, a percentage of its surface is protected, without specifying which part is protected. The weapon effects

¹² Taken from http://en.wikipedia.org/wiki/Bulletproof_vest#Performance_standards.

model uses this percentage to determine the amount of ballistic damage on the whole surface. This means that SCOPE has no notion of things like head-protection or ballistic plates protecting parts of the torso. The effect of protection is distributed over the whole surface area of the entity, resulting in a lower (chance of) damage to the entity. The next section describes the weapon effects model implemented in SCOPE.

5.3 Weapon Effects

Weapon effects are, as many other aspects in SCOPE, probability based: Not the actual damage done by one particular bullet is calculated, but the probable amount of damage from an amount of bullets. Where other simulations perform a statistical analysis over many different possible encounters, SCOPE will directly calculate the average outcome of those possible encounters. In other words: When it has been determined that a bullet has a 10% chance of being a lethal shot, the target will be 10% damaged (closer to death). This direct calculation of average outcomes has some clear advantages (no need for repeated runs, completely deterministic behaviour), but is not straightforward to implement for an essentially discrete event such as a gunfight. This section will first describe how the threat of powers is calculated and then explain how this is used to determine average damage.

5.3.1 Threat

The calculation of threat is influenced by several factors: the weapon, the target (e.g. protection), cover, etcetera. The first factor is the accuracy with which the threat is delivered.

5.3.1.1 Accuracy

The aiming value for weapons with the best sights is in the order of 1 to 3 arcmin. If the target is moving this may increase to 15 arcmin. If the aimer is moving, shivering or panting while aiming, this has a similar effect on the accuracy. When both move, the effects are additive. The accuracy is a parameter that has to be provided for each weapon and sight pair. The absolute error σ increases with the distance between shooter and target:

$$\sigma = \text{aiming} \cdot \text{distance}$$

5.3.1.2 Geometry

The geometry for threat exertion is governed by three parameters:

- τ is the action range of the power (from the delivery point).
- σ is the inaccuracy with which the power is applied.
- ε is the size of the target.

With these parameters we discern six cases:

Precise powers:

- I $\tau < \sigma < \varepsilon$: the target is large compared to the action range and inaccuracy, a certain hit. The power has a short action range (e.g. laser beam, stabbing).
- II $\sigma < \tau < \varepsilon$: the target is large compared to the action range and inaccuracy, a certain hit. The action range exceeds the inaccuracy (e.g. pepper spray, water cannon).

Surface powers:

- III $\varepsilon < \sigma < \tau$: the action range exceeds the inaccuracy, a certain hit. Not so accurately delivered (e.g. PsyOps leaflets, chemical agents).
- IV $\sigma < \varepsilon < \tau$: the action range exceeds the inaccuracy, a certain hit. Accurately delivered (e.g. mines).

Probabilistic powers:

V $\tau < \epsilon < \sigma$: the inaccuracy exceeds target size and action range, a probabilistic hit.
The power has a short action range (e.g. a bullet).

VI $\epsilon < \tau < \sigma$: the inaccuracy exceeds target size and action range, a probabilistic hit.
The action range is larger than the target (e.g. grenades, air burst).

In order to find a common formula for these cases we consider the area where the threat may land and compare that to the area where the threat will actually affect the target. The first area is a circle with radius $\epsilon + \sigma$ around the centre of the target. The second is a circle with the radius $\epsilon + \tau$ around the centre of the target. When $\epsilon + \sigma < \epsilon + \tau$, some potentially harmful threats will never occur, since no threats are delivered outside the $\epsilon + \sigma$ border. The harmful radius is thus limited to the minimum of $\epsilon + \sigma$ and $\epsilon + \tau$. This results in the following formula, the ratio of the surfaces of the two circles:

$$p = \frac{(\epsilon + \min(\tau, \sigma))^2}{(\epsilon + \sigma)^2}.$$

This simple result for all cases is further moderated by at least two factors. The first is that obstacles in the terrain may provide cover to the target. This allows him to limit his exposure, if he is risk aware. And when not risk aware, he might be covered by chance. The other factor is that an action range for *fragmenting powers* gives the reach of the fragments, but not the density.

5.3.1.3 *Cover*

Cover is provided by objects in the terrain. We discern the typical size p (m) and the density D (objects/m²). The chance that an object at distance d to $d + \Delta d$ blocks the line to the target is:

$$\Delta p = \Delta d D \rho.$$

The chance on a blocked angle for a distance up to d is $p(d)$ and thus:

$$p = 1 - e^{-D \rho d},$$

with $-D \rho$ the cover factor. For inhomogeneous terrain, the cover factor may vary over the path. In that case the cover can be calculated as the arithmetic average over the segments:

$$\exp(-cover_1 d_1) \exp(-cover_2 d_2) \dots \exp(-cover_n d_n) =$$

$$\exp(-cover \cdot d), \text{ with}$$

$$cover = \frac{(cover_1 d_1 + cover_2 d_2 + \dots + cover_n d_n)}{d_1 + d_2 + \dots + d_n}, \text{ and}$$

$$d = \sum_{i=1}^n d_i$$

5.3.1.4 *Indirect powers*

For fragmenting indirect powers, the density of the fragments must be calculated to determine the threat. Suppose that N_f is the number of fragments, passing through a hemisphere of $2\pi/2$ area. The target has a surface area of $\pi^3 \epsilon$ and catches $N_f \epsilon^2 / 2r^2$ particles on average. Due to interception by cover, this number is reduced to:

$$A(r) = \frac{N_f \epsilon^2 \exp(-cover \cdot r)}{2r^2}$$

We assume any hit is an incapacitation of the target. If the target is armoured this is effectuated by adjusting ϵ . If the number of fragments exceeds 1, the target is incapacitated for sure, if it is lower it represents the chance of incapacitation:

$$\text{if } A(r) \geq 1 \text{ then } q(r) = 1 \text{ else } q(r) = A(r)$$

The chance to be incapacitated by the fragmenting power is then the surface weighted average of all r , up to the action range. In the case of $\sigma > \tau$, the action range is τ , but if $\tau > \sigma$, the limit is σ . The integration limit is thus $\min(\sigma, \tau)$:

$$P(\epsilon, \tau) = \frac{\int_{r=0}^{\min(\sigma, \tau)} 2\pi r q(r) dr}{\pi \min(\sigma, \tau)^2} \Leftrightarrow$$

$$P(\epsilon, \tau) = \frac{2}{\pi \min(\sigma, \tau)^2} \int_{r=0}^{\min(\sigma, \tau)} r q(r) dr$$

$P(\epsilon, \tau)$ is called the threat density. The final threat is then:

$$Threat = p \cdot P = \frac{(\epsilon + \tau)^2}{(\epsilon + \sigma)^2} P(\epsilon, \tau).$$

For non-fragmenting threats, such as a single bullet, high explosive, flame, etcetera, the particle concept is irrelevant. This results in a definition of $q(r)$ with only the extinguishing part of cover:

$$q(r) = \exp(-cover \cdot r),$$

$$P(\epsilon, \tau) = \frac{2}{\min(\sigma, \tau)^2} \int_{r=0}^{\min(\sigma, \tau)} r q(r) dr$$

5.3.1.5 Direct Powers

Direct powers work mostly geometrically the same as indirect powers (see Section 5.3.1.4) with two exceptions, both resulting from the fact that the position of the shooter is coincidental with the delivery point. The first is that the effect of the cover factor of the terrain should be calculated over the distance d between shooter and target, rather than the radius r between delivery point and target. The other is that the integration of chances.

5.3.2 Damage

The previous section detailed how one shot (e.g. bullet, grenade or beam) exerts its threat to the target. But engagements in SCOPE are between entities that (usually) consist of several individuals. This section describes the method by which the effects of single shots is integrated into the total damage.

Damage to an entity is continuous and should be interpreted as fatal casualties. This leads to counter intuitive results such as fractional group sizes. A group size of 2.5 should be interpreted as describing that some possible outcomes resulted in group sizes of 2 or less, while other outcomes lead to group sizes of 3 or more. This is the result of the SCOPE

philosophy of directly calculating the average outcome. The total damage is determined in several steps, collecting the detailed information from the threat model into more generalised damage results.

The function `calcIncapChance` is the top-level function, collecting the data necessary to calculate the damage. The first step is determining the individual positions of all individuals in both entities, the source and the target. In SCOPE we assume that each individual in the source entity engages each individual in the target entity with equal probability. The second assumption SCOPE uses is that all weapons in the group have an equal probability to be used by each group member. That means that for each position the chance that a particular weapon is used is the same, summing to a total of 1.0. The next version of SCOPE might use a more sophisticated method, see the section Future Work for more details on this. The result of these steps is a set of engagements between the individuals of the source entity and the target entity with a number of different weapons.

The function `calcIncapChanceOfWeaponOverTime` is used to calculate the damage done by an individual using one weapon engaging one target. As indicated by the function name this function deals with the timing aspects of firing a weapon. If the response time of the used weapon is longer than the time the target is exposed, no shots are fired and no damage is done. After the response time of the weapon, the first shot is fired, followed by as many shots as the repeat rate allows, given the exposed time. Within SCOPE only one shot of a series can damage the target, so the chance that a shot hits the target is calculated by multiplying the chance of a hit with the chance that the previous shots missed the target. A continuous weapon (gas, beam) results in a certain hit, when the exposed time exceeds the response time, of course.

This result is further modulated to include the effect of the source being in cover. Being in cover limits the effectiveness of firing, which is reflected in a lower chance to damage the target.

The function `calcIncapChanceOfWeapon` is used to perform the calculations as described in the section Threat. This function returns the chance that a shot actually damages a target. This is the lowest level function in the calculation of the damage. In the top-level function `calcIncapChance`, the results from the underlying functions are combined to return the combined and weighted effect of firing all weapons at all individuals in the target. Several weight factors have to be applied to normalise the total sum. The returned chance reflects the damage done by firing all weapons at all individuals in the target by all individuals in the source over a given period of time. But the period of time is only available once, so we have to multiply by the probability that a certain individual in the source engaged a certain individual in the target with one weapon. Assuming equal probability for all choices, we just calculate the average outcome. When the size of the source entity is n individuals and the target size is m , we have a normalisation factor of $1/(n \cdot m)$ to normalise for the group sizes. Normalisation for the number of weapons is a little bit more complex, since in SCOPE only one weapon can do damage in a hit, so each next weapon is weighted by the chance of the previous weapons missing the target.

5.3.3 Assessing Damage

As well as the functions `calcIncapChance` the functions `assessIncapChance` and `assessIncapRisk` have been implemented. These functions perform a more efficient calculation of the incapacitation chance, while sacrificing some accuracy. Within these functions the position of the individuals is simplified to the centre of mass of the entities, so the engagements between all individuals can be calculated in one go. The extra function `assessIncapRisk` makes a *worst case* estimate of the

incapacitation chance. To calculate this estimate it takes as argument the exposed area of the target entity, rather than calculating it from the values in the target object that is also passed as an argument to the function. This allows the calculation of the incapacitation chance (risk) with a different exposed area than the actual exposed area, e.g. a greater exposed area to reflect the risk when *not* in cover. What's more, the `assessIncapRisk` function doesn't factor in the effect of the source being in cover. When a source is in cover the incapacitation chance is lowered, but this is not the case when the (worst case) incapacitation risk is estimated, it assumes the incapacitation chance of a source not in cover. This is used in the perceived threat function for entities. The perceived threat is used for the threat perception (see the section on Threat perception), where an entity estimates its risk of being shot. When an entity is in cover, it should estimate the risk of being shot while *not* in cover. This will then be the motivation for staying *in* cover.

5.4 Future Work

As mentioned in the previous section Damage, an engagement is equally spread out over both entities (source and target). This randomness should become a bit more structured. Sources should engage the most exposed target individual and the damage within an entity should be collected at the level of individuals. This will lead to more realistic results such as the individual in the foremost position or with the least cover being the first to be eliminated. Now the damage of an engagement is equally distributed over individuals that are at positions with bad cover and the individuals with good cover or individuals that are out of range.

Implementing such a scheme would mean attaching some sort of damage buckets to individuals in the target entity. This is complicated by the fact that an entity doesn't have a concept of individuals, just positions taken from the formation. Splitting entities into individuals is a deviation from the SCOPE philosophy, but should probably be implemented for engagements.

6 References

- Belyavin, A.J. & Spencer, M.B. (2004),
Modeling performance and alertness: the QinetiQ approach,
Aviat Space Environ Med 75 (3, Suppl.): A93-A103.
- Bonen, A.; Campbell, C.J.; Kirby, R.L. & Belcastro, A.N. (1979),
A multiple regression model for blood lactate removal in man,
Pflügers Archiv European Journal of Physiology, 380(3): 205-210.
- De Bruin, R.; Verwijs, C. & Van Vliet, A.J. (2007),
Mental inzetbaarheid van teams: ontwikkeling van een model van teamfunctioneren als
module voor SCOPE, Report TNO-DV 2007 A140,
Soesterberg: TNO Defence, Safety and Security.
- Dubois, D. & Dubois, E.F. (1916),
Clinical calorimetry X: Formula to estimate the appropriate surface area if height and
weight be known,
Archiv. Internal Med 17, 863-871.
- Engel, F.L. (1971),
Visual conspicuity. Directed attention and retinal locus,
Vision Research 11, 563-575.
- EUR 18957 (1999),
COST Action 231, Digital mobile radio towards future generation systems, final report,
tech. rep.; European Communities.
- Gagge, A.P.; Stolwijk, J.A.J. & Nishi, Y. (1971),
An effective temperature scale, based on a simple model of human physiological
regulatory response,
ASHRAE Trans 74, 242 - 262.
- Griffith, J. (1997),
Test of a model incorporating stress, strain and disintegration in the cohesion-
performance relation,
Journal of Applied Social Psychology, 27, (17), 1489-1526.
- Guyton, A.C. & Hall, J.E. (2000),
Textbook of Medical Physiology,
W.B. Saunders.
- Hargreaves, M. (2004),
Muscle glycogen and metabolic regulation,
Proc Nutrit Soc 63, 217-220.
- Havenith, G. (1997),
Individual heat stress response, Thesis,
Univ Nijmegen, ISBN 90-9010979-X.
- Hersey, P.; Blanchard, K.H. & Johnson, D.E. (1996),
Management of Organizational Behavior (7th ed.),
Englewood Cliffs, NJ: Prentice Hall.
- Hogervorst, M.A.; Toet, A. & Bijl, P. (2005),
On the relationship between Human search strategies, conspicuity and search
performance,
SPIE Proc 5784-31, 240-251.

- Itti, L. & Koch, C. (1999),
Comparison of feature combination strategies for saliency-based visual attention systems,
Proceedings of SPIE - The International Society for Optical Engineering 3644, pp. 473- 482.
- Itti, L.; Koch, C. & Niebur, E. (1998),
A model of saliency-based visual attention for rapid scene analysis,
IEEE Transactions on Pattern Analysis and Machine Intelligence; 20(11);1254-1259V.
- Jehn, K.A.; Northcraft, G.B. & Neale, M.A. (1999),
Why differences make a difference: A field study of diversity, conflict and performance in workgroups,
Administrative Science Quarterly, 44, 741-763.
- Lotens, W.A. (1978),
Criteria for maximal tolerable thermal load,
Report TNO Institute for Perception, TM 1978-13.
- Lotens, W.A. (1993),
Heat transfer from humans wearing clothing. Thesis,
Delft University of Technology.
- Mori, T. (1985),
Visual conspicuity of a moving dot, horizontal line segment or vertical line segment,
Vision Res 25 (8), 1083-1088.
- Nilsson L.H. (1973),
Liver glycogen content in man in the postabsorptive state,
Scand J Clin Lab Invest., 32(4): 317-23.
- Nothdurft, H.C. (1993),
The conspicuousness of orientation and motion contrast,
Spat Vis 7(4), 341-363.
- Nothdurft, H.C. (2000),
Saliency from feature contrast: additivity across dimensions,
Vision Res 40 (10-12), 1183-1201.
- O'Kane, B.L. & Page, G.L. (2006),
Figure of merit for predicting detection of moving targets,
Optical Eng 45 (9), 096402.
- Okumura, Y.; Ohmori, E.; Kawano, T. & Fukuda, K. (1968),
Field Strength and Its Variability in VHF and UHF Land-Mobile Radio Service,
Review of the Electrical Communication Laboratory.
- Oliver, L.W.; Harman, J.; Hoover, E.; Hayes, S.M. & Pandhi, N.A. (1999),
A quantitative integration of the military cohesion literature,
Military Psychology, 11(1), 57-83.
- Rollinson, D. & Broadfield, A. (2002),
Organisational behaviour and analysis: An integrated approach 2nd ed.,
New York: Prentice Hall Financial Times.
- Selfridge, O.G. (1959),
Pandemonium: a Paradigm for Learning. Proc. Symposium on Mechanization of Thought Processes: National Physical Laboratory,
London: HM Stationery Office.

- Stolwijk, J.A.J. (1971),
A mathematical model of physiological temperature regulation in man,
NASA Contractor Report CR-1855, Washington DC.
- Toet, A.; Kooi, F.L.; Bijl, P. & Valetton, J.M. (1998),
Visual conspicuity determines human target acquisition performance,
Opt. Eng. 37 (7), 1969–1975.
- Van Vliet, A.J.; Van Amelsfoort, D.J.C. & Van Bommel, I.E. (2004),
Inzetbaarheid Personeel, Report TM-04-A060,
Soesterberg: TNO Defence, Security and Safety.

7 Signature

Soesterberg, April 2008

TNO Defence, Security and Safety

A handwritten signature in black ink, consisting of a series of loops and a long horizontal stroke extending to the right.

Prof. Dr H.A.M. Daanen
Head of department

A handwritten signature in black ink, featuring a stylized 'E' and 'U' followed by a horizontal stroke.

E.M. Ubink, MSc
Author

ONGERUBRICEERD
REPORT DOCUMENTATION PAGE
(MOD-NL)

1. DEFENCE REPORT NO (MOD-NL) TD2008-0050	2. RECIPIENT'S ACCESSION NO -	3. PERFORMING ORGANIZATION REPORT NO TNO-DV 2008 A126
4. PROJECT/TASK/WORK UNIT NO 032.13114	5. CONTRACT NO -	6. REPORT DATE April 2008
7. NUMBER OF PAGES 59 (excl RDP & distribution list)	8. NUMBER OF REFERENCES 30	9. TYPE OF REPORT AND DATES COVERED Draft
10. TITLE AND SUBTITLE Models & Methods in SCOPE A status report		
11. AUTHOR(S) E.M. Ubink, MSc Dr W.A. Lotens R.F. Aldershoff, MSc		
12. PERFORMING ORGANIZATION NAME(S) AND ADDRESS(ES) TNO Defence, Security and Safety, P.O. Box 23, 3769 ZG Soesterberg , The Netherlands Kampweg 5, 3769 DE, Soesterberg, The Netherlands		
13. SPONSORING AGENCY NAME(S) AND ADDRESS(ES) Dutch Ministry of Defence, P.O. Box 20701, 2500 ES, The Hague		
14. SUPPLEMENTARY NOTES The classification designation Ongerubriceerd is equivalent to Unclassified, Stg. Confidentieel is equivalent to Confidential and Stg. Geheim is equivalent to Secret.		
15. ABSTRACT (MAXIMUM 200 WORDS (1044 BYTE)) SCOPE is a simulation of dismounted soldier operations developed by TNO. SCOPE is used for research in the field of operational performance. Operational performance depends on many factors, varying from climate and terrain characteristics to group dynamics and equipment. SCOPE contains models and variables representing many of these factors. This report is a status overview of the models and variables that are currently implemented in SCOPE.		
16. DESCRIPTORS Operational simulation, Behaviour, Situation Awareness, Physiology, weapon effects.		IDENTIFIERS Human performance modelling, dismounted soldier operations.
17a. SECURITY CLASSIFICATION (OF REPORT) Ongerubriceerd	17b. SECURITY CLASSIFICATION (OF PAGE) Ongerubriceerd	17c. SECURITY CLASSIFICATION (OF ABSTRACT) Ongerubriceerd
18. DISTRIBUTION AVAILABILITY STATEMENT Unlimited Distribution		17d. SECURITY CLASSIFICATION (OF TITLES) Ongerubriceerd

ONGERUBRICEERD

Distribution list

The following agencies/people will receive a complete copy of the report.

- | | |
|-------|---|
| 1 | DMO/SC-DR&D
standaard inclusief digitale versie bijgeleverd op cd-rom |
| 2/3 | DMO/DR&D/Kennistransfer |
| 4 | Programmabegeleider Defensie
(inclusief digitale versie bijgeleverd op cd-rom)
Mindef/DMO/DP&V/Ressort Projecten/Bureau SMP
lkol J. Kerkhof |
| 5 | Projectbegeleider Defensie
(inclusief digitale versie bijgeleverd op cd-rom)
Mindef/DS/CLAS/OTCO/OTCMan
maj H.J. van den Brink |
| 6/8 | Bibliotheek KMA |
| 9 | Programmaleider TNO Defensie en Veiligheid
dr. ir. A.A. Woering |
| 10/14 | TNO Defensie en Veiligheid, vestiging Soesterberg,
drs. R. de Bruin
dr. A.J. van Vliet
dr. W.A. Lotens
drs. R.F. Aldershof
drs. E.M. Ubink |
| 15/20 | TNO Defensie en Veiligheid, vestiging Den Haag
drs. R.R. Barbier
ir. C. Fiamingo
M.B. Heebing
ir. M. Spaans
ir. P.P.J. de Krom
ir. R.R. Witberg |

Onderstaande instanties/personen ontvangen het managementuittreksel en de distributielijst van het rapport.

4 ex.	DMO/SC-DR&D
1 ex.	DMO/ressort Zeesystemen
1 ex.	DMO/ressort Landsystemen
1 ex.	DMO/ressort Luchtsystemen
2 ex.	BS/DS/DOBBP/SCOB
1 ex.	MIVD/AAR/BMT
1 ex.	Staf CZSK
1 ex.	Staf CLAS
1 ex.	Staf CLSK
1 ex.	Staf KMar
1 ex.	TNO Defensie en Veiligheid, Algemeen Directeur, ir. P.A.O.G. Korting
1 ex.	TNO Defensie en Veiligheid, Directie Directeur Operaties, ir. C. Eberwijn
1 ex.	TNO Defensie en Veiligheid, Directie Directeur Kennis, prof. dr. P. Werkhoven
1 ex.	TNO Defensie en Veiligheid, Directie Directeur Markt, G.D. Klein Baltink
1 ex.	TNO Defensie en Veiligheid, vestiging Den Haag, Manager Waarnemingssystemen (operaties), ir. B. Dunnebier PDeng
1 ex.	TNO Defensie en Veiligheid, vestiging Den Haag, Manager Informatie en Operaties (operaties), ir. P. Schulein
1 ex.	TNO Defensie en Veiligheid, vestiging Rijswijk, Manager Bescherming, Munitie en Wapens (operaties), ir. P.J.M. Elands
1 ex.	TNO Defensie en Veiligheid, vestiging Rijswijk, Manager BC Bescherming (operaties), ir. R.J.A. Kersten
1 ex.	TNO Defensie en Veiligheid, vestiging Soesterberg, Manager Human Factors (operaties), drs. H.J. Vink